REPORT DOCUMENTATION PAGE

Form Approved
OMB No. 0704-0188

PLEASE DO NOT RETURN YOUR FORM TO THE ABOVE ORGANIZATION.

1. REPORT DATE *(DD-MM-YYYY)*	2. REPORT TYPE	3. DATES COVERED *(From - To)*
22-02-2010	Final Performance Report	From 01-03-07 to 30-11-2007

4. TITLE AND SUBTITLE
Insect Optic Glomeruli: exploration of a universal circuit for sensorimotor processing

5a. CONTRACT NUMBER

5b. GRANT NUMBER
FA9550-07-1-0230

5c. PROGRAM ELEMENT NUMBER

6. AUTHOR(S)
Olberg, Robert, M

5d. PROJECT NUMBER

5e. TASK NUMBER

5f. WORK UNIT NUMBER

7. PERFORMING ORGANIZATION NAME(S) AND ADDRESS(ES)
Union College Center Corporation
Trustees of Union College
807 Union Street
Schenectady, NY 12308-3103

8. PERFORMING ORGANIZATION REPORT NUMBER

9. SPONSORING/MONITORING AGENCY NAME(S) AND ADDRESS(ES)
Air Force Office of Scientific Research
875 N. Randolph Street, Room 3112
Arlington, VA 22203-1768

10. SPONSOR/MONITOR'S ACRONYM(S)
AFOSR

11. SPONSOR/MONITOR'S REPORT NUMBER(S)
AFRL-SR-AR-TR-10-0109

12. DISTRIBUTION/AVAILABILITY STATEMENT

DISTRIBUTION A: Approved for Public Release

13. SUPPLEMENTARY NOTES
Grant Co-PIs: Strausfeld, Nicholas, J, Department of Neuroscience, University of Arizona
Higgins, Charles, M, Department of Electrical Engineering, University of Arizona

14. ABSTRACT

Electrophysiological investigations of dragonfly target-selective descending neurons yielded the following findings:(1) Outdoor experiments with 2 families of dragonflies with different prey capture strategies revealed family-specific differences in the receptive fields. (2) Real objects moving in 3 dimensions elicited greater responses to nearby small objects than predicted from responses to images on a flat visual display. (3) Outdoor experiments and experiments with expanding images on a flat display revealed looming-object preference of 2 TSDNs, which appear to predict time-to-contact. (4) TSDNs showed extremely high spike rates with the raised body temperatures (30°-35°C) seen in naturally behaving dragonflies. (5) Two TSDNs were tuned to looming objects, coding for time-to-contact. (6) Two TSDNs were identified whose spikes carry predictive information about future object position. Investigation of flight behavior revealed that take-off direction is a linear function of the prey's angular velocity 28 ms before takeoff. Collaboration with Dr. Anthony Leonardo (HHMI-JFRC) led to development of a flight arena, a chronic electrode implantation technique, and a miniature telemetry chip, paving the way for wireless recording of TSDN activity during prey interception.

15. SUBJECT TERMS
INSECT VISION, FLIGHT, INTERCEPTION, DRAGONFLY

16. SECURITY CLASSIFICATION OF:			17. LIMITATION OF ABSTRACT	18. NUMBER OF PAGES	19a. NAME OF RESPONSIBLE PERSON
a. REPORT	b. ABSTRACT	c. THIS PAGE			Olberg, Robert M.
U	U	U	UU	33	19b. TELEPHONE NUMBER *(Include area code)* 518-388-6509

Reset

Objectives

The principle objectives of the project addressed by the Olberg laboratory were to determine the nature of the information extracted by insect optic glomeruli, specifically in the dragonfly. Dragonflies were deemed to be ideal for this study for the following 3 reasons.

(1) As large aerial predators, they are ideally suited to the behavioral quantification of object discrimination and tracking. The dragonfly will reliably take off to pursue flying objects, and its large size and low wing beat frequency allows us to capture the entire event with very high spatial and temporal resolution, resolving, for example, the orientation of the head and other body parts in free flight.

(2) The speed of the dragonfly's prey-capture behavior necessitates very rapid visual processing and information transmission, resulting in the evolution of large neurons subserving these functions, large neurons that are unusually accessible for microelectrode studies.

(3) The predictive nature of prey interception and capture makes this an ideal system in which to examine the higher order visual motion processing likely to take place, at least in part, in the optic glomeruli.

The results of the investigations in the Olberg lab during the granting period included the following:

(1) Outdoor experiments with 2 families of dragonflies that pursue different prey capture strategies revealed family-specific differences in the receptive fields of the target-selective descending neurons (TSDNs).

(2) Responses of TSDNs to real objects moving in 3 dimensions showed greater responses to nearby small objects than predicted from responses to images on a flat visual display.

(3) Outdoor experiments and experiments with expanding images on a flat display revealed looming-object preference of 2 TSDNs, which appear to predict time-to-contact.

(4) The TSDNs showed extremely high spike rates with the raised body temperatures seen in naturally behaving dragonflies.

(5) Composite position and direction receptive fields revealed for the first time the coverage of the stimulus space by the TSDNs.

(6) Outdoor recordings confirmed an earlier finding that two TSDNs carry predictive information about future target position.

(7) High-speed video analysis of prey interception flights revealed that take-off direction is a linear function of the prey's angular velocity approximately 28 ms before takeoff.

(8) Collaboration with Anthony Leonardo at Janelia Farm led to development of a flight arena, a chronic electrode implantation technique, and a miniature telemetry chip, paving the way for wireless recording of TSDN activity during prey interception.

Background

A brief summary of the visual control of foraging flight by dragonflies is included here to make the results presented below more comprehensible. Dragonflies can be divided into 2 groups based on their aerial foraging strategy. "Hawkers" (mostly family Aeshnidae) fly nearly continuously from dawn to dusk, actively foraging from the wing. "Perchers" (most members of the other dragonfly families, especially Libellulidae) are sit-and-wait predators, foraging from a perch such as a reed, rock, or log. The behavioral studies to date were restricted to perchers of the family Libellulidae. The following description of the behavior has emerged.

1. Before takeoff the dragonfly accurately assesses the distance to the target (Olberg et al 2005).
2. The dragonfly takes off in a direction that leads the target (Olberg et al. 2000 and in preparation).
3. After takeoff the dragonfly steers an interception course, continuously correcting for changes in the target's trajectory (Olberg et al. 2000).
4. During the interception flight, the dragonfly's head rotates to fixate the target on the "crosshairs" formed by the horizontal dorsal fovea and the vertical midline (Olberg et al. 2007).
5. The legs are extended for capture 20 ms before contact with the prey (Worthington and Olberg, in preparation).

Eight pairs of large visual interneurons, called Target Selective Descending Neurons (TSDNs) descend in the ventral nerve cord (VNC) from the brain to flight control centers of the thoracic ganglia. Because they are highly selective for the motion of small objects, and because their activity elicits small steering movements of the wings, the TSDNs are implicated in controlling the prey-interception flight. What is known about the TSDNs provides a partial explanation for some, but not all of the above points about the behavior. Because the small-target selective TSDNs are strongly directionally selective and their activity elicits steering movements of the wings, their activity is likely to account for course corrections during pursuit (point 3). The TSDNs transmit nearly as much information about target position as target velocity. Interestingly the positional information provided by some of the TSDNs is more tightly correlated with the future position of the target than with its present position (Adelman et al. 2003), suggesting a role in the course prediction necessary for intercepting the moving prey (points 2 & 4). Two of the TSDNs respond most strongly to approaching, i.e. looming, objects. Their spike timing provides accurate time-to-contact information, with bursts about 100 ms before an expanding image makes virtual contact (point 5) over a wide range of object sizes and approach speeds. Dragonflies accurately assess prey distance before takeoff (point 1 -- Olberg et al., 2005). It is believed that motion parallax, induced by head movement, is the basis for this distance estimation. However,

nothing is known at present about the neuronal circuitry involved in distance estimation in dragonflies.

Results and Development during the granting period

Electrophysiology in the natural environment

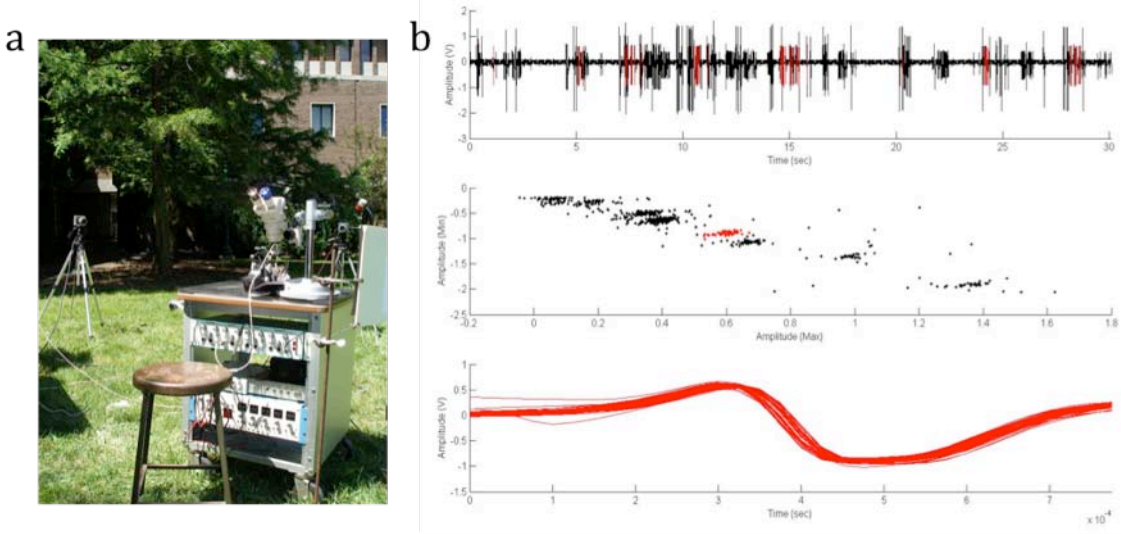

Figure 1. a. Mobile electrophysiology rig for outdoor experiments. In the background are 2 high-speed video cameras on tripods, for 3-D reconstruction of the hand-delivered visual stimulus. b. Example of a spike trace from the mobile rig. Clusters in middle panel are individual TSDNS (example in red in middle and lower panels.

To fully understand the extraction of visual information by the TSDNs it was necessary to study the system under the conditions in which it has evolved to operate. Although it is desirable to recreate these conditions in a controlled laboratory environment (see below) an important first step was to record TSDN responses outdoors in warm summer conditions under blue skies, the only conditions under which the dragonfly forages naturally (Fig 1).

Briefly, dragonflies of two families, Aeshnidae and Libellulidae, were immobilized, dorsal side up. TSDNs were recorded extracellularly with a suction electrode applied to the dorsal surface of one connective of the ventral nerve cord posterior to the prothoracic ganglion. Target stimuli, 2mm, 4mm, and 8mm white beads affixed to a taut fine nylon monofilament stretched on wood dowel bow, were moved by hand in a pseudorandom path around the animal. Bead movement was recorded with 2 high-speed video cameras for subsequent 3-dimensional reconstruction. (The TSDNs showed no responses to control tests with monofilament lacking beads or to wide-field striped grating patterns.) Spiking data was recorded (40 KHz sampling), sorted (Fig 1b), and correlated

with the stimulus bead movement. Of 14 outdoor preparations, 6 gave useful data, 3 from Aeshnid dragonflies (*Aeshna canadensis*) and 3 from Libellulid dragonflies (*Pachydiplax longipennis*). The large data sets obtained allowed resolution of receptive fields at a much higher resolution than has been achieved before. Individual TSDNs were identified by their amplitudes and by previous characterizations of receptive fields and directional preferences obtained from intracellular recording and dye injections. The data also yielded information on the depth dimension of receptive field, on responses to approaching and receding targets, on responses to objects of different absolute size, on variation of responses with ambient temperature, on responses to target speed, on temporal coupling of spikes among TSDNs, and on prediction of future target location.

Receptive-field studies

Three-dimensional fields were obtained for 7 TSDNs in both Aeshnid and Libellulid dragonflies. In many cases, the data confirmed earlier lab results, but with much greater resolution. However there were also many new findings, and some findings that contradicted earlier work. The most important findings are summarized here.

Contrary to previously published results (Frye and Olberg 1995), the present study determined that the large MDT3 receptive field is located ipsilateral to the connective in which its axon descends (Fig 2). Recent laboratory experiments with intracellular recording and dye injection have confirmed this finding. Although MDT3 showed directional preference for upward movement, it was more broadly tuned directionally than all but one other TSDN, DIT3. This may be explained by the fact that these two neurons, MDT3 and DIT3, showed consistent, robust looming responses to approaching objects (see "*Looming responses*" section below). The response to approaching objects was reflected in the high density of spiking to bead movement near the animal (Fig 2, lower left panel).

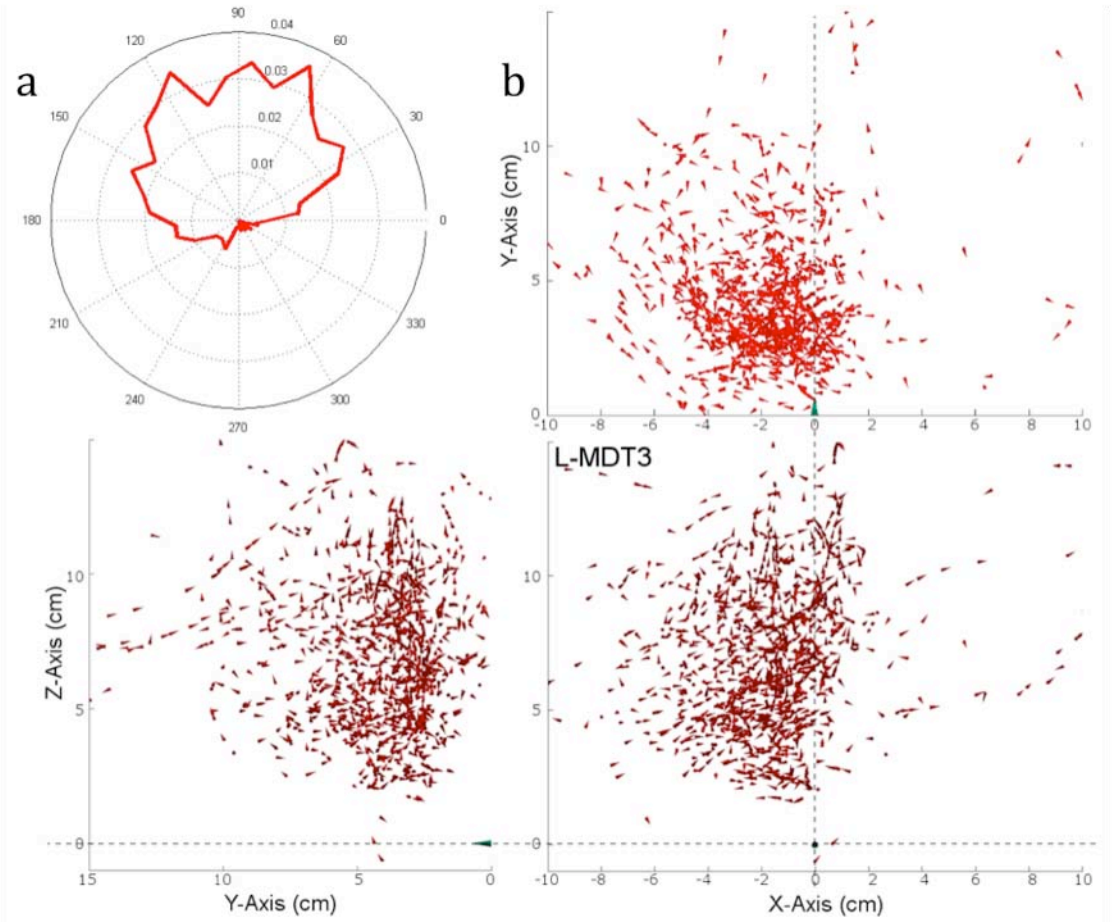

Figure 2. Receptive field of MDT3 in the left connective of an Aeshnid dragonfly a. Normalized circular histogram of spike-correlated bead directions. b. Scatterplot of spike-correlated bead positions viewed from the top (above), front (below right) and side (below left). Red cones represent bead position and direction of the bead at each spike time. Large green cones at (0,0,0) indicate the position and direction of the dragonfly's head.

Two TSDNs, MDT4 and DIT1, were especially selective for small targets. Both had relatively small receptive fields, roughly centered on visual midline (Figs 3, 4, & 6). The three-dimensional stimulus presentation revealed a previously unknown difference in their size selectivity. MDT4 showed a consistent preference for small (2°-4°) targets, responding to all 3 bead sizes but preferring small beads closer and larger beads farther away (Fig 5). DIT1, however, showed a preference for larger targets in both angular and absolute terms, while still responding to small targets (Fig 7). An intriguing possibility is that once a small target image is acquired, the DIT1 shifts its size preference to continue responding as the target draws nearer. Modulation of size preference for an approaching object would be consistent with locking onto an approaching prey item, suggesting the sort of higher order properties that could be mediated by the optic glomeruli.

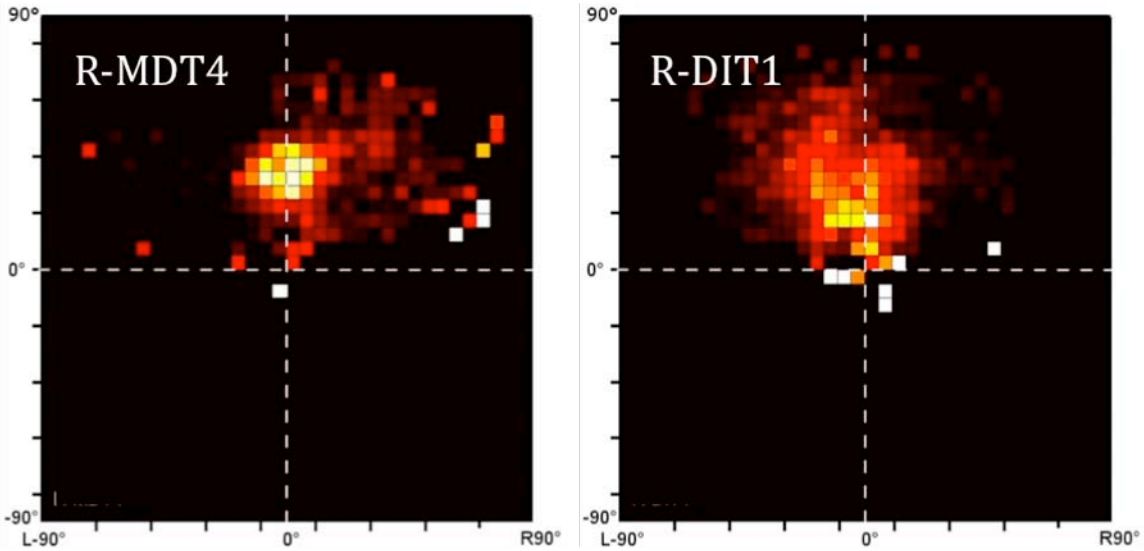

Figure 3. Normalized receptive fields, in angular coordinates of 2 TSDNs in Aeshnid dragonflies. Each bin represents a 5°x5° region of space viewed from the dragonfly's perspective. Data was normalized by dividing the spikes per bin over the number of times that bin was sampled by the moving bead.

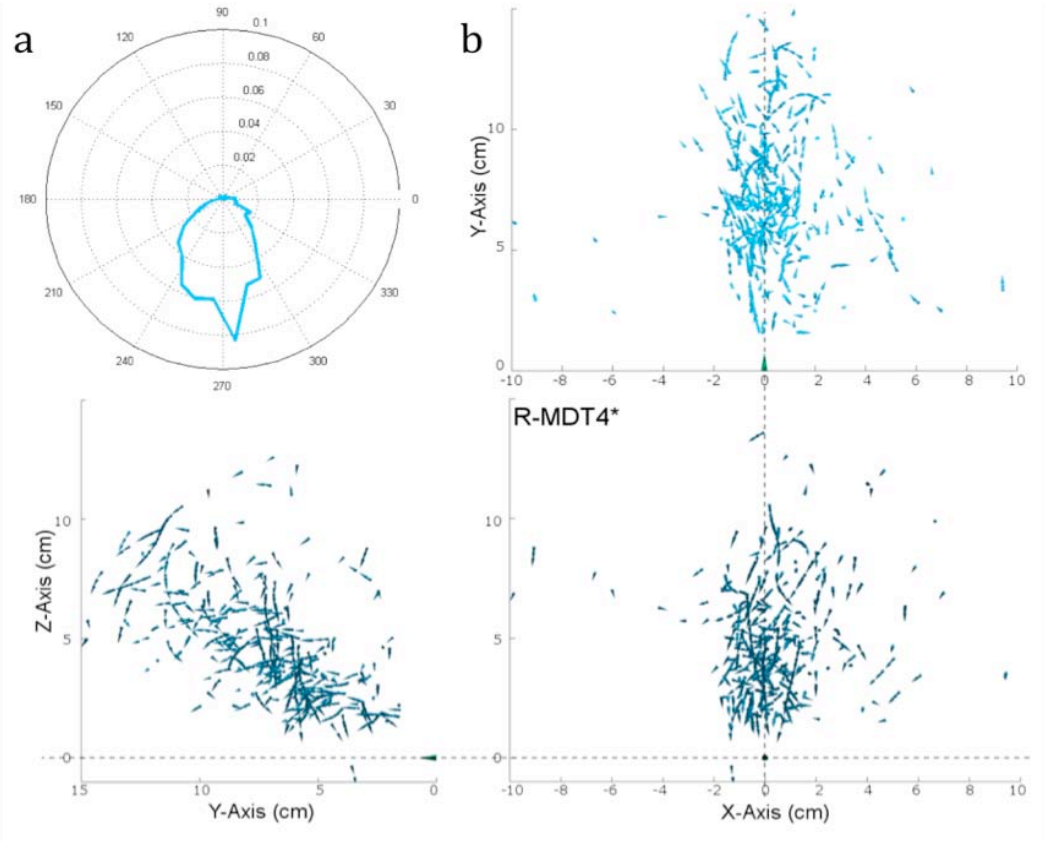

Figure 4. Receptive field of MDT4 in the right connective of an Aeshnid dragonfly a. Normalized circular histogram of spike-correlated bead directions. b. Scatterplot of spike-correlated bead positions viewed from the top (above), front (below right) and side (below left). Light blue cones represent bead position and direction of the bead at each spike time. Large green cones at (0,0,0) indicate the position and direction of the dragonfly's head.

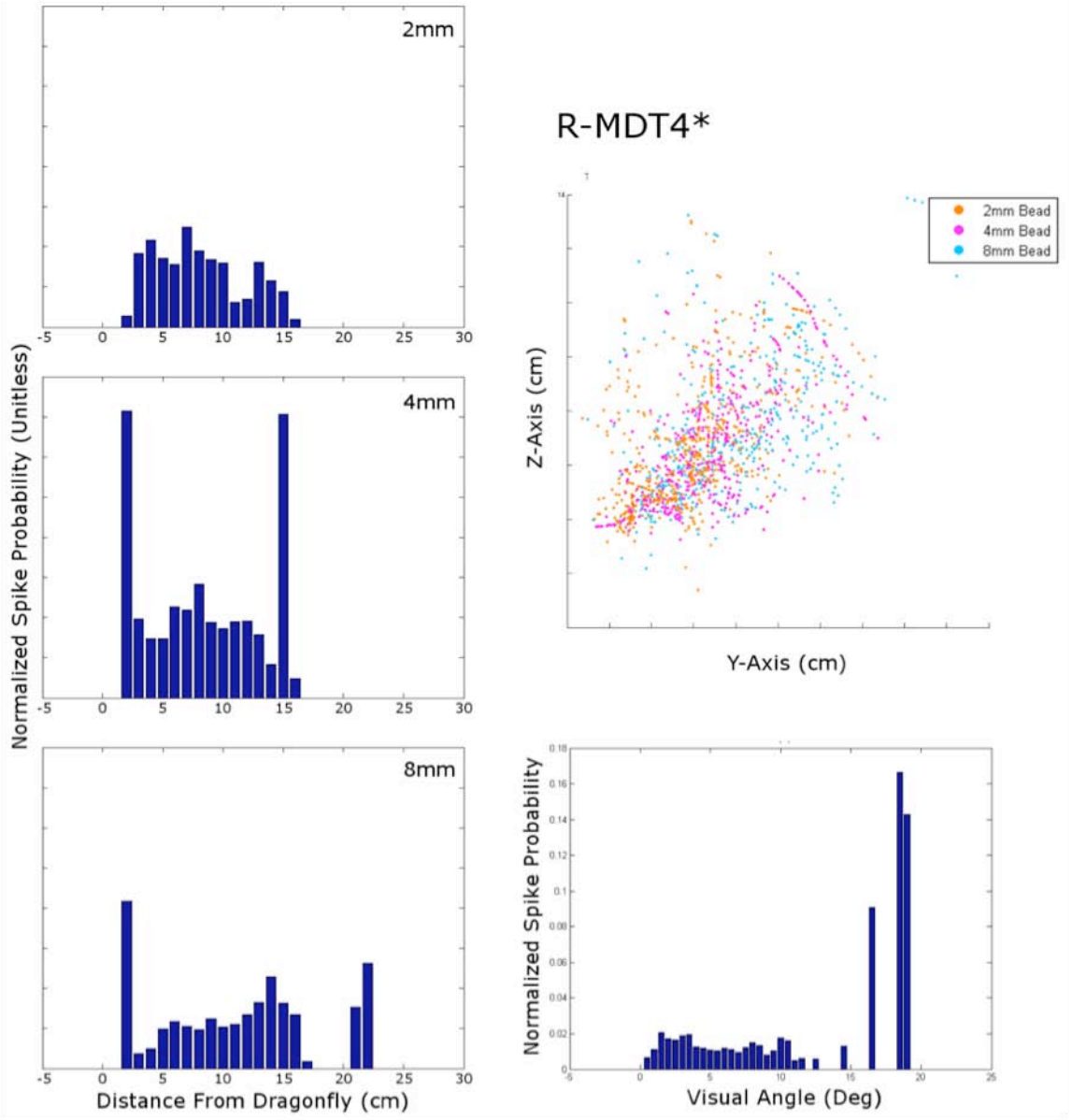

Figure 5. Size and distance preferences of MDT4 in an Aeshnid dragonfly. a. Normalized histograms of bead distance from the dragonfliy's head for each MDT4 spike. b. Scatterplot of spike-correlated bead locations, viewed from the side. Orange – 2 mm bead, Magenta – 4 mm bead, Cyan – 8 mm bead. c. Normalized histogram of bead target angle correlated with MDT4 spikes.

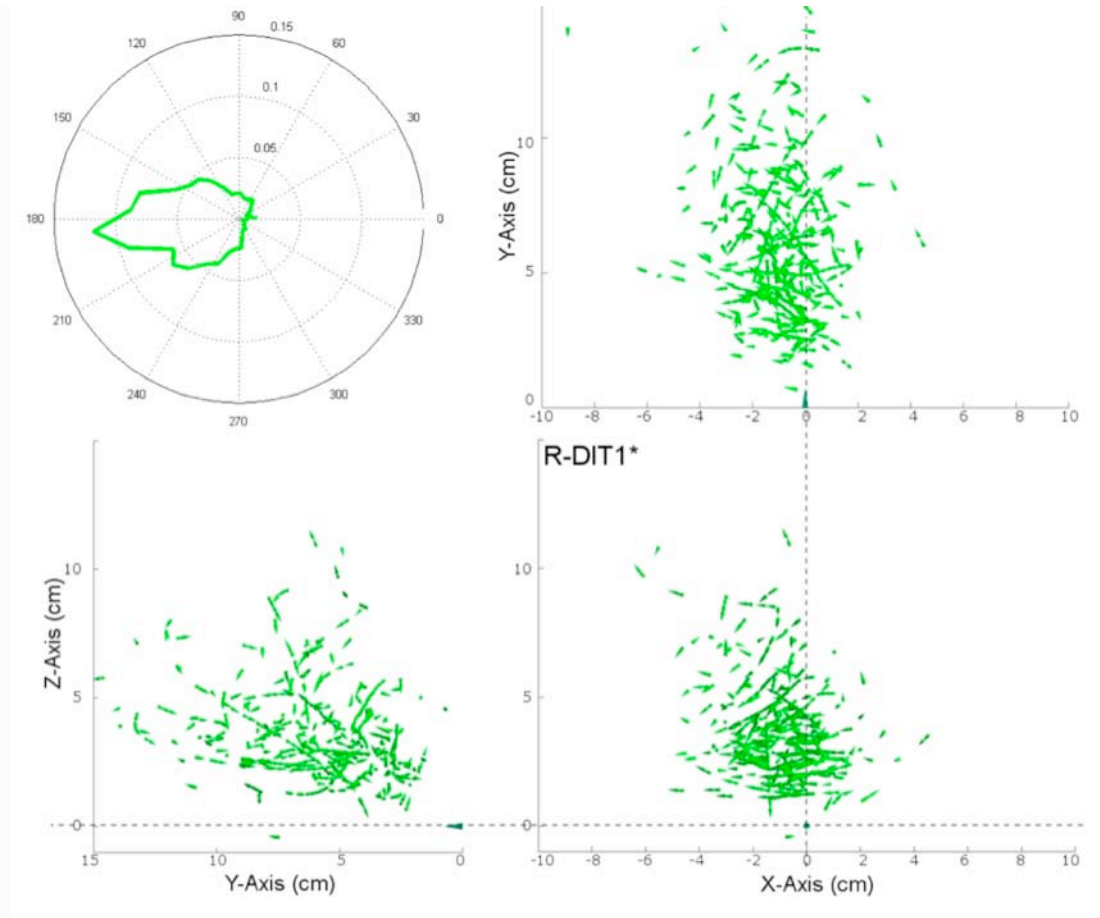

Figure 6. Receptive field of DIT1in the right connective of an Aeshnid dragonfly a. Normalized circular histogram of spike-correlated bead directions. b. Scatterplot of spike-correlated bead positions viewed from the top (above), front (below right) and side (below left). Bright green cones represent bead position and direction of the bead at each spike time. Dark green cones at (0,0,0) indicate the position and direction of the dragonfly's head.

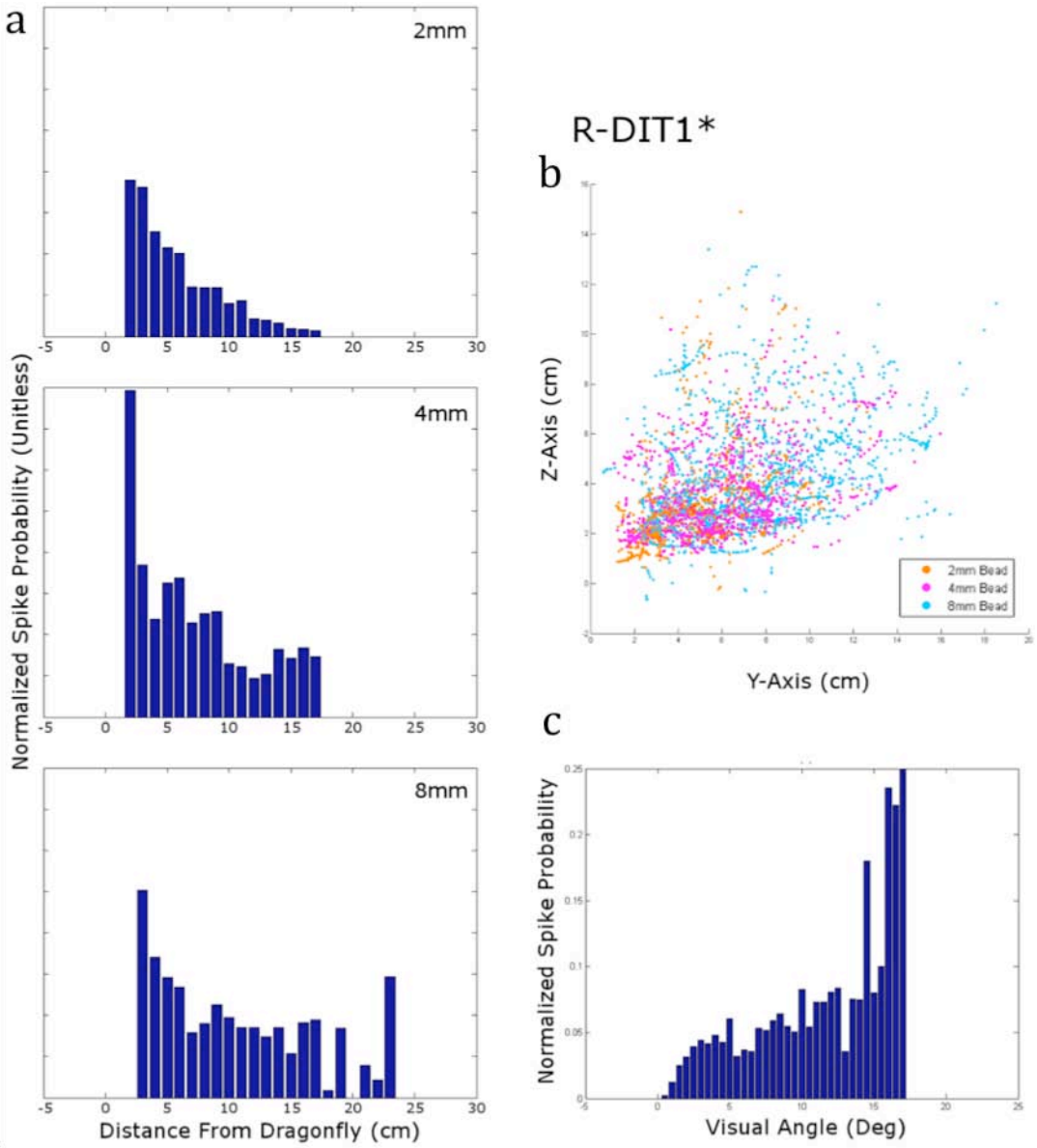

Figure 7. Size and distance preferences of DIT1 in an Aeshnid dragonfly. a. Normalized histograms of bead distance from the dragonfliy's head for each DIT1 spike. b. Scatterplot of spike-correlated bead locations, viewed from the side. Orange – 2 mm bead, Magenta – 4 mm bead, Cyan – 8 mm bead. c. Normalized histogram of bead target angle correlated with MDT4 spikes.

Some consistent differences were discovered between the TSDN receptive fields in Aeshnids and those in Libellulids. An example of these can be seen by comparing the DIT3 receptive field in an Aeshnid (Fig 8) to that in a Libellulid (Fig 9). DIT3 in the Aeshnid had a monocular (contralateral) receptive field, whereas DIT3 in the Libellulid had a much larger binocular (contralaterally weighted) receptive field. Aeshnids are "hawking" predators, foraging from the wing, and Libellulids are perching predators taking off after prey. This

difference seen in TSDN properties could reflect the differences in the prey interception flights and their roles in guiding that behavior.

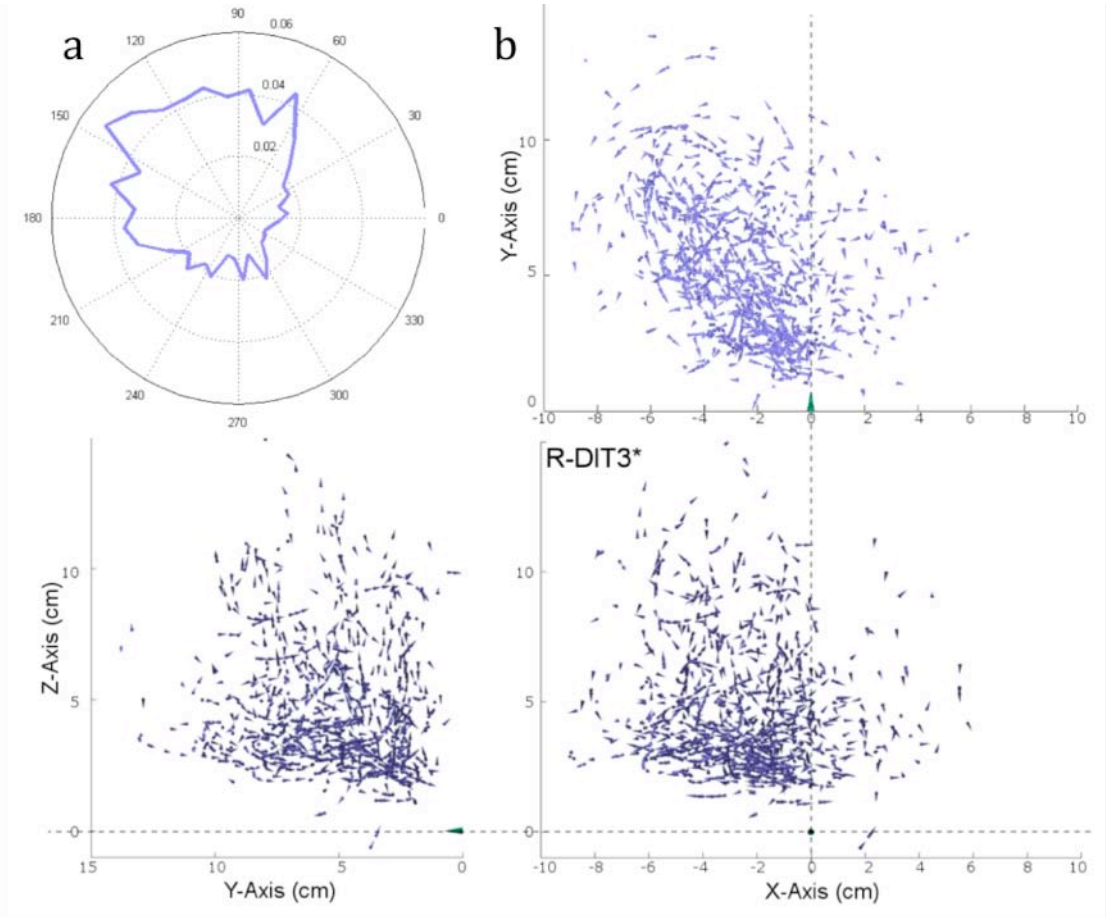

Figure 8. Receptive field of DIT3 in the right connective of an Aeshnid dragonfly a. Normalized circular histogram of spike-correlated bead directions. b. Scatterplot of spike-correlated bead positions viewed from the top (above), front (below right) and side (below left). Violet cones represent bead position and direction of the bead at each spike time. Dark green cones at (0,0,0) indicate the position and direction of the dragonfly's head.

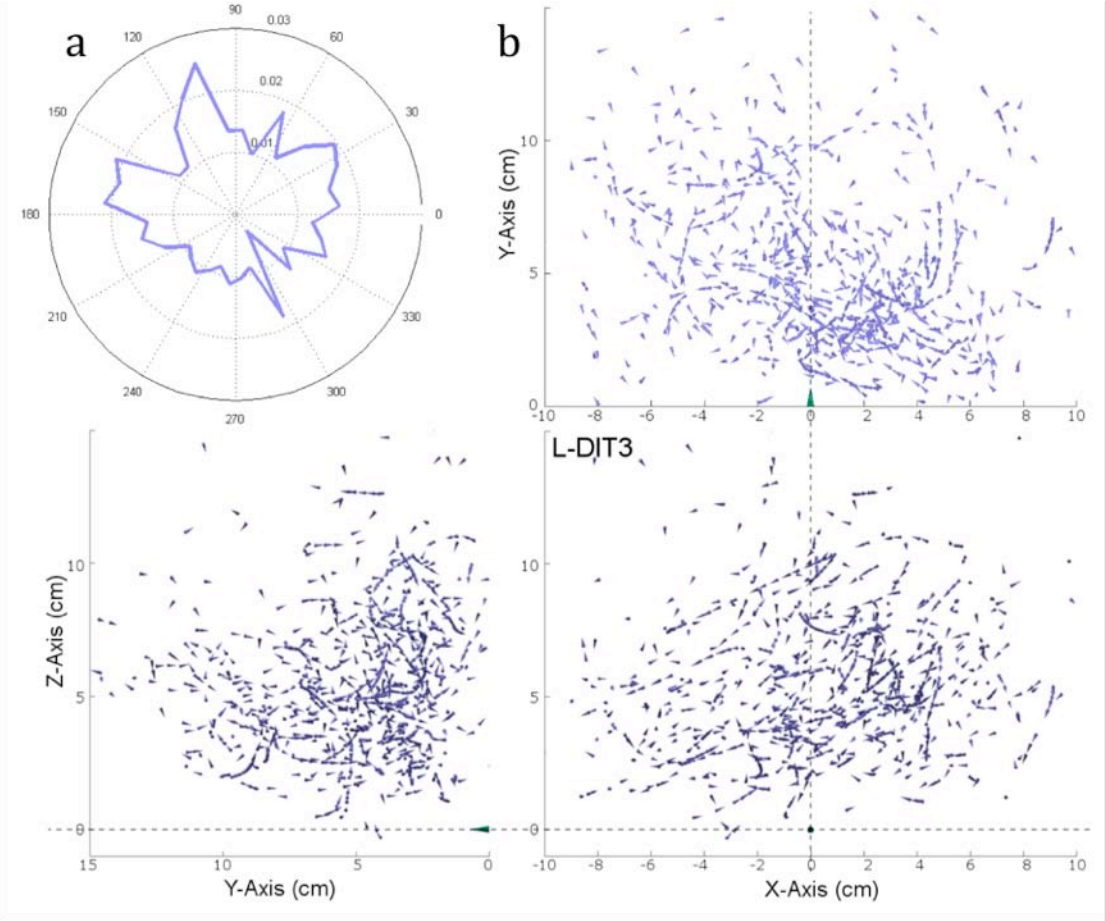

Figure 9. Receptive field of DIT3 in the left connective of an Libellulid dragonfly a. Normalized circular histogram of spike-correlated bead directions. b. Scatterplot of spike-correlated bead positions viewed from the top (above), front (below right) and side (below left). Violet cones represent bead position and direction of the bead at each spike time. Dark green cones at (0,0,0) indicate the position and direction of the dragonfly's head.

The DIT3 recordings in both Aeshnids and Libellulids showed a strong preference for nearby objects and larger target sizes (Fig 10 shows an example from Aeshnids). Spiking probability was histogrammed as a function of the component vector of bead motion directly toward or away from the dragonfly's head. DIT3 in both Aeshnids and Libellulids showed a strong preference for approaching objects and smaller responses to receding objects (Fig 11). These results were consistent with the hypothesized role of DIT3 (and MDT3) in detecting looming objects and signaling the time to contact (see "*Looming response*" section below).

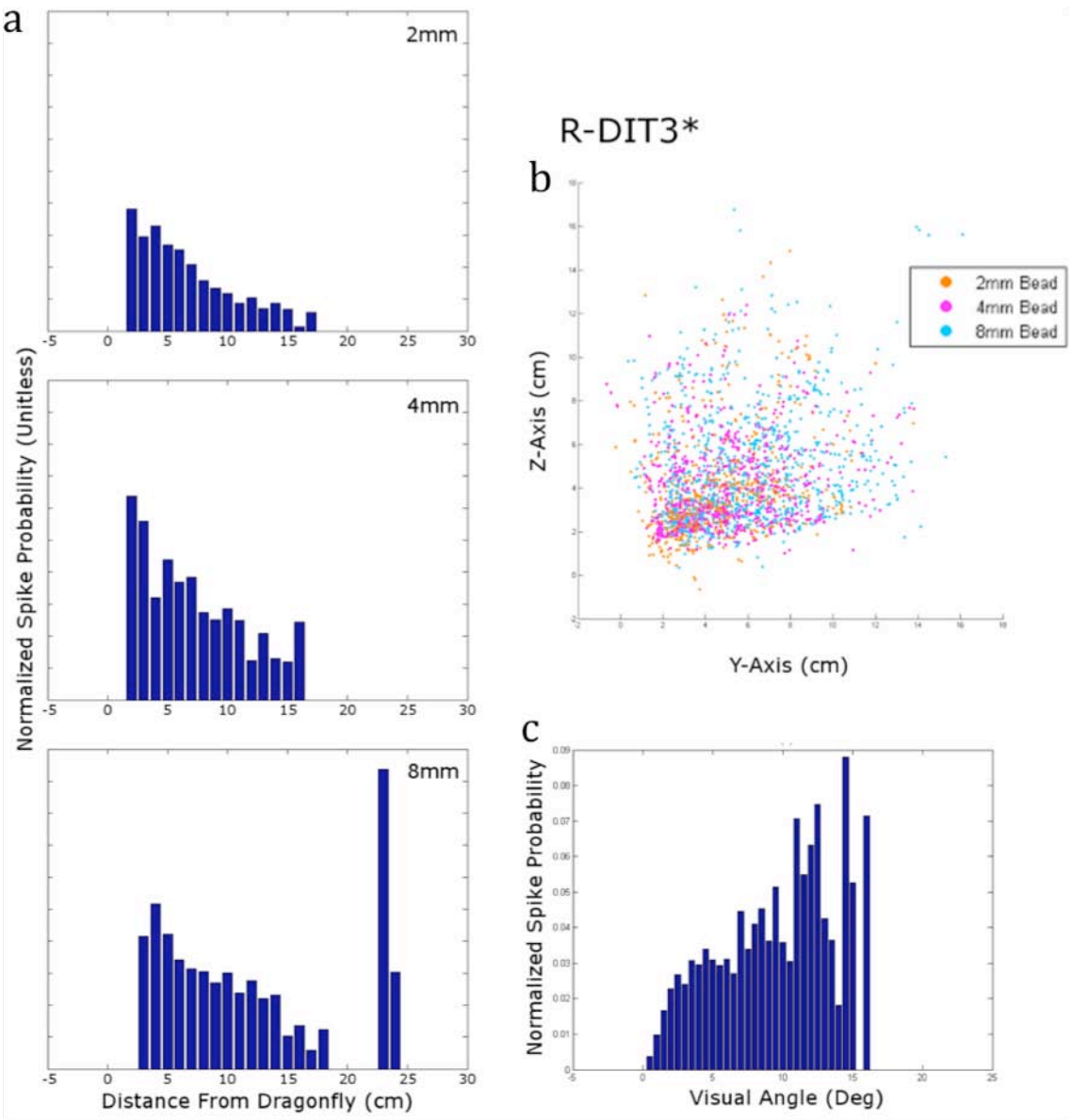

Figure 10. Size and distance preferences of DIT3 in an Aeshnid dragonfly. a. Normalized histograms of bead distance from the dragonfliy's head for each DIT3 spike. b. Scatterplot of spike-correlated bead locations, viewed from the side. Orange – 2 mm bead, Magenta – 4 mm bead, Cyan – 8 mm bead. c. Normalized histogram of bead target angle correlated with MDT4 spikes.

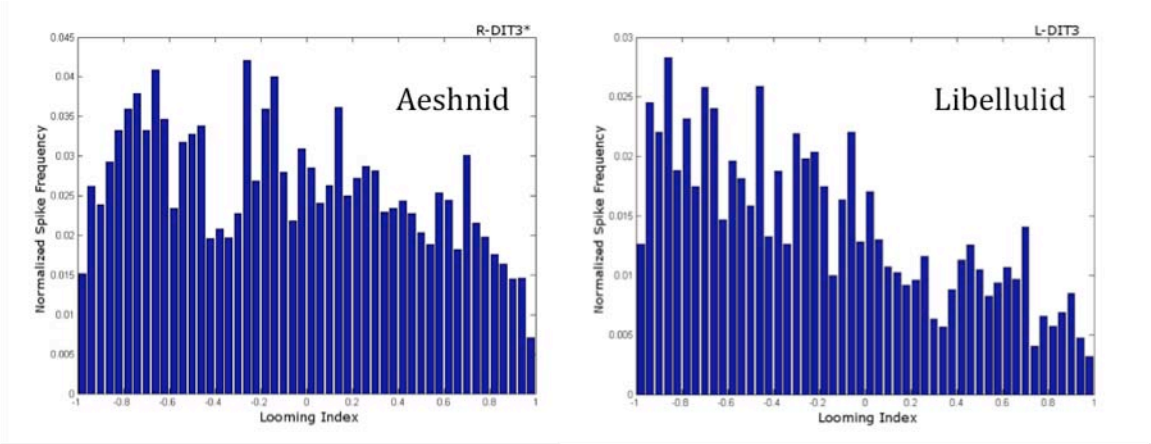

Figure 11. Looming index for DIT3 in Aeshnid and Libellulid dragonflies. For each spike the instantaneous change in r (head-bead distance) was divided by the instantaneous change in angular speed. Values of -1, 0, and 1 correspond to movement directly towards, tangential, and directly away from the head, respectively.

In the outdoor suction-electrode experiments, all the neurons were recorded in the same animal with a consistent head position and head angle for all. Because of that, the multiunit extracellular recordings allowed a better understanding of relative receptive field coverage and directional preferences of the TSDNs than was previously available. A summary diagram for the 5 TSDNs that were strongly directionally selective (all but the 2 looming-sensitive neurons, MDT3 and DIT3) is shown in figure 12a. An overlay of polar plots of directional sensitivity (Fig 12b) showed that any direction of target motion can be represented by a combination of the responses of two TSDNs. Interestingly the directional curves are orthogonally arrayed and aligned either with the horizontal or the vertical. DIT2 was not included in this overlay; its directional preference was indistinguishable from that of MDT2. (Note: Fig 12a depicts the receptive fields of TSDNs in the right connective, whereas Fig 12b depicts directional curves of TSDNs in the left connective.)

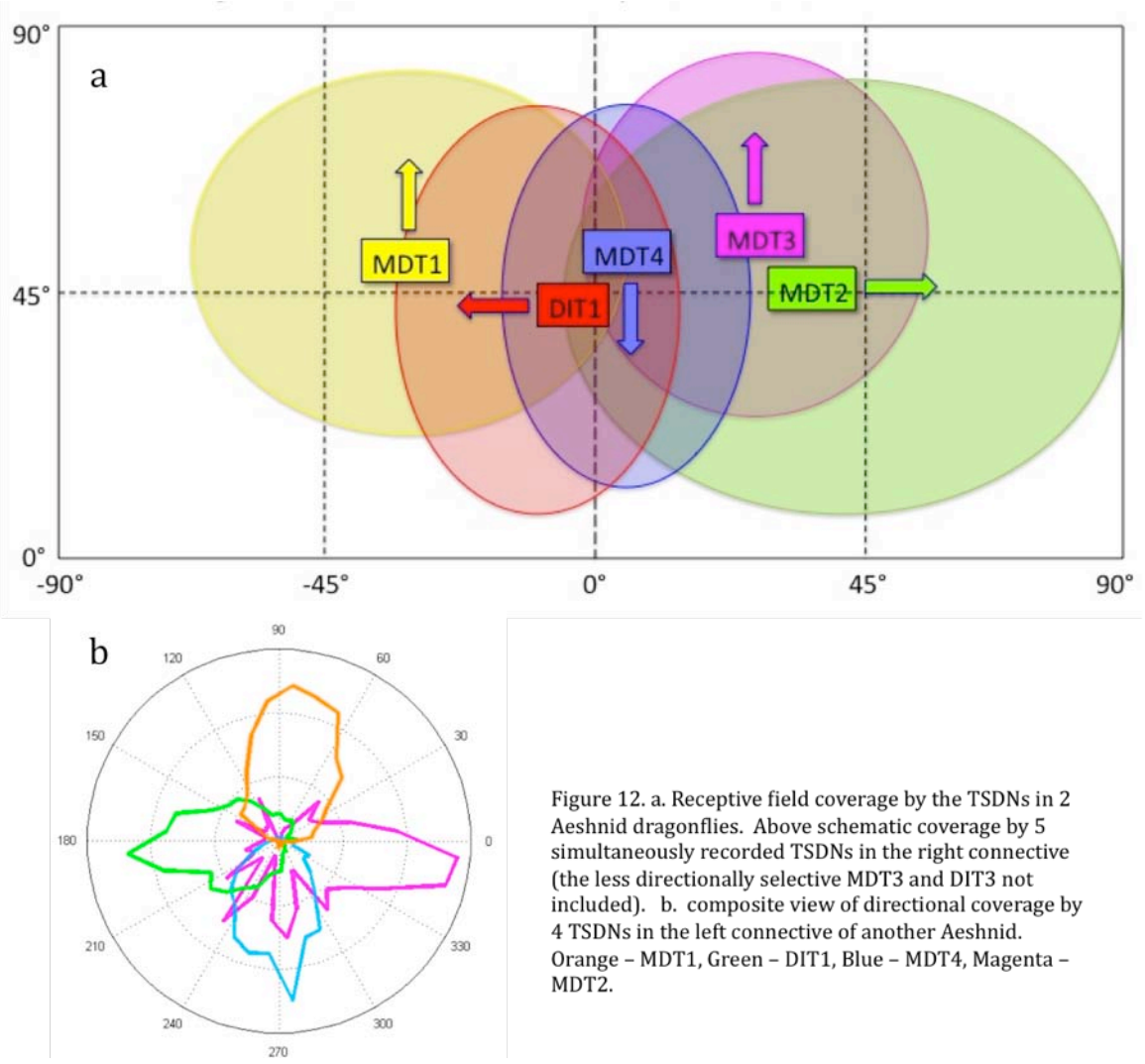

Figure 12. a. Receptive field coverage by the TSDNs in 2 Aeshnid dragonflies. Above schematic coverage by 5 simultaneously recorded TSDNs in the right connective (the less directionally selective MDT3 and DIT3 not included). b. composite view of directional coverage by 4 TSDNs in the left connective of another Aeshnid. Orange – MDT1, Green – DIT1, Blue – MDT4, Magenta – MDT2.

Light level and temperature

An obvious difference in the TSDN responses between the outdoor and laboratory recordings was in the overall level of spike activity. Instantaneous spike frequencies approaching or even exceeding 1 KHz were not uncommon in the outdoor experiments, whereas spike frequencies over 250 Hz were rare in previous laboratory experiments.

There were several possible explanations for the elevated activity level. The two most likely of these were light level and temperature. Light levels were approximately 2 orders of magnitude higher from the blue sky in the outdoor experiments than from the 240 Hz CRT monitor used in earlier laboratory experiments (240 μmol of photons)/m2/s vs. 3.4 μmol of photons)/m2/s). Ambient temperature during the outdoor experiments was also much higher than in the lab (outdoor expts 24°-30° C, indoor experiments 20°-23° C).

Furthermore peak spike frequencies were much higher on hotter days outdoors than on cooler days (Fig. 13).

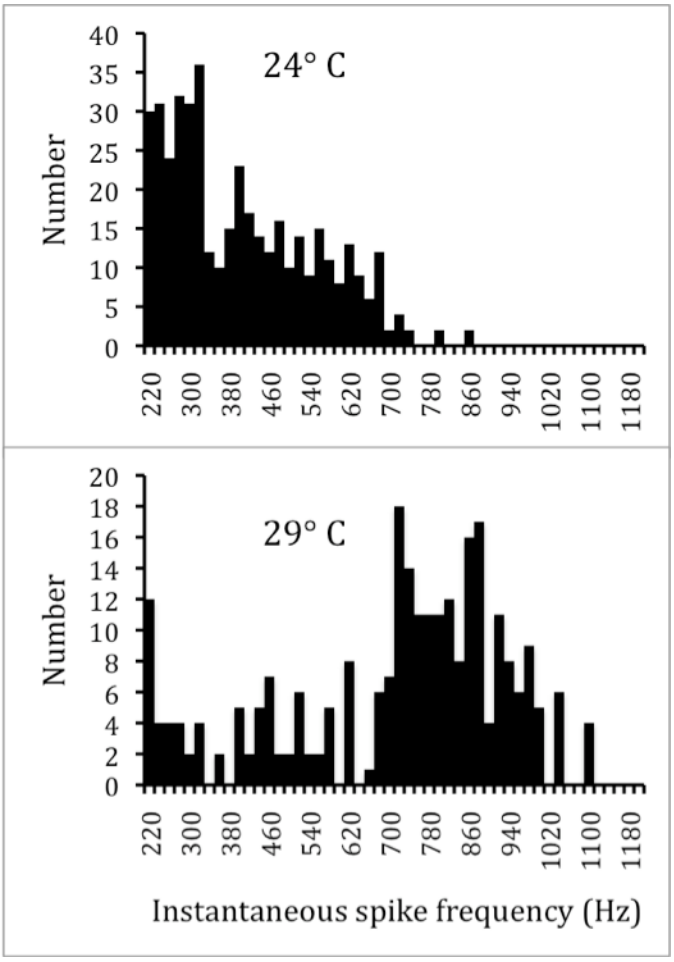

Figure 13. Frequency histograms of MDT1 in 2 Libellulid dragonflies, recorded at 2 different ambient temperatures. Plotted are spike frequencies (reciprocals of interspike intervals) above 200 Hz.

To increase light level in laboratory experiments, a DLP projector (120 Hz Lightspeed, by DepthQ) has been adapted for visual stimulus presentation. The projector was modified by removing the color wheel so that the code for successive stimulus frames was addressed to the R, G, and B channels, using custom software developed by Dr. Anthony Leonardo. The modified projector thus produced 360 Hz updates and with an irradiance (measured 1 cm from the transmission screen) of 465 μmole/m^2/s, slightly higher than typical light levels from blue sky illumination and more than 100 times the irradiance of the previously used CRT display.

The effect of body temperature on TSDN responses was investigated using the newly modified 360 Hz projector. The results of these pilot experiments confirmed that high light levels combined with body temperatures of at least 30° C are sufficient to elicit spiking responses comparable to those seen outdoors. These experiments also showed that at elevated body temperature TSDNs

responded to targets that elicited no response at lower body temperatures (Fig. 14).

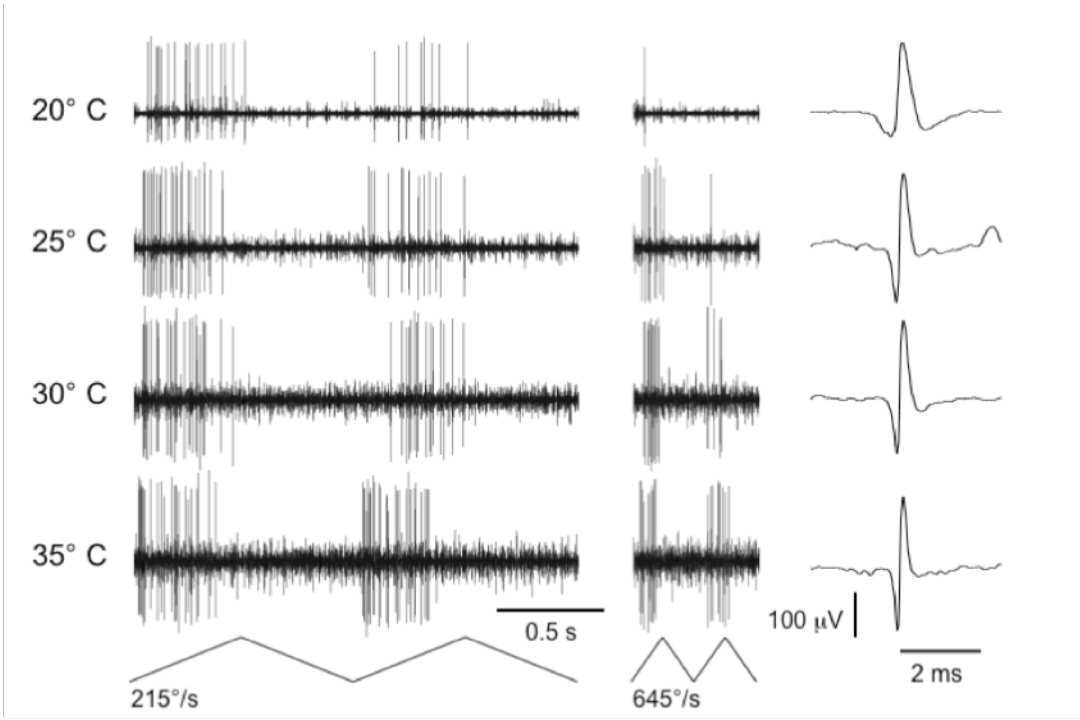

Figure 14. Effect of temperature on response of a TSDN (not identified) to up and down movement of 2° target. Note that at 20° body temperature there was little or no response to the higher speed target movement, which elicited robust spiking at body temperatures above 30°. Individual spikes at right show progressive spike narrowing with temperature.

Looming responses

Using intracellular microelectrodes and fluorescent dye injection (Lucifer Yellow CH), two undergraduates in the Olberg lab with AFOSR grant support, Kaitlyn Tagarelli and Ritu Shah, studied the looming responses of TSDNs in Libellulid dragonflies. The stimulus was an expanding circular target on a 240 Hz monochrome CRT monitor, where the time course of expansion simulated an object approaching at a constant speed. Of 75 intracellular recordings of large visual descending interneurons in Libellulid dragonflies, 10 were classified as looming sensitive. Four of these recordings were identified as being from DIT3 and 5 as being from MDT3, based on both anatomical and physiological criteria. One of the recordings was too short to make a determination of its identity. In some cases a looming white circle was presented against a dark background. This stimulus also elicited looming responses in both DIT3 (Fig 15) and MDT3. An expanding black and white checkerboard-filled circle, whose expansion caused no change in mean luminance also elicited the spiking responses in both neurons, implying that the responses were to expansion and not to luminance changes (Fig 15).

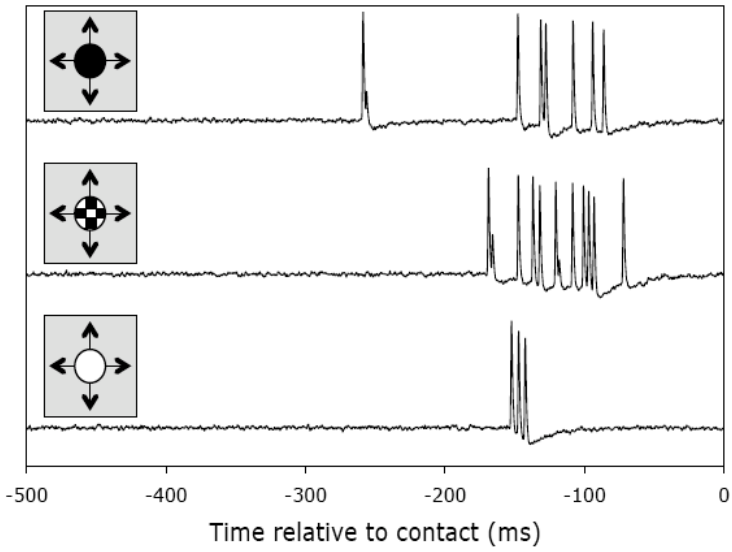

Figure 15. Responses of looming-sensitive neuron, DIT3, in a Libellulid dragonfly to expanding circular targets whose time course of expansion simulated approaching objects. This neuron responded to image expansion whether the expansion resulted in net dimming (a), brightening (c), or no net light intensity change (b). Stimulus: **a,c**. 1.7 cm target approaching 1 m/s on axis from 50 cm directly in front. **b,** 1.7 cm target approaching 1 m/s on axis from 1 m directly in front.

Both DIT3 and MDT3 showed a robust and consistently timed response to expanding images whose time-course of expansion followed that of angular expansion of an object moving (Fig. 16). Specifically, both neurons responded to looming stimuli with a burst of spikes approximately 100 to 150 ms before the simulated approaching object would contact the animal's head. This was true for virtual objects of a variety of sizes (1-5 cm diameter, Fig 16) even though the time course of image expansion varied greatly. There was no consistent difference between the firing times of DIT3 (Fig 16b) and MDT3 (Fig 16c), but, in general, DIT3 produced more spikes than MDT3.

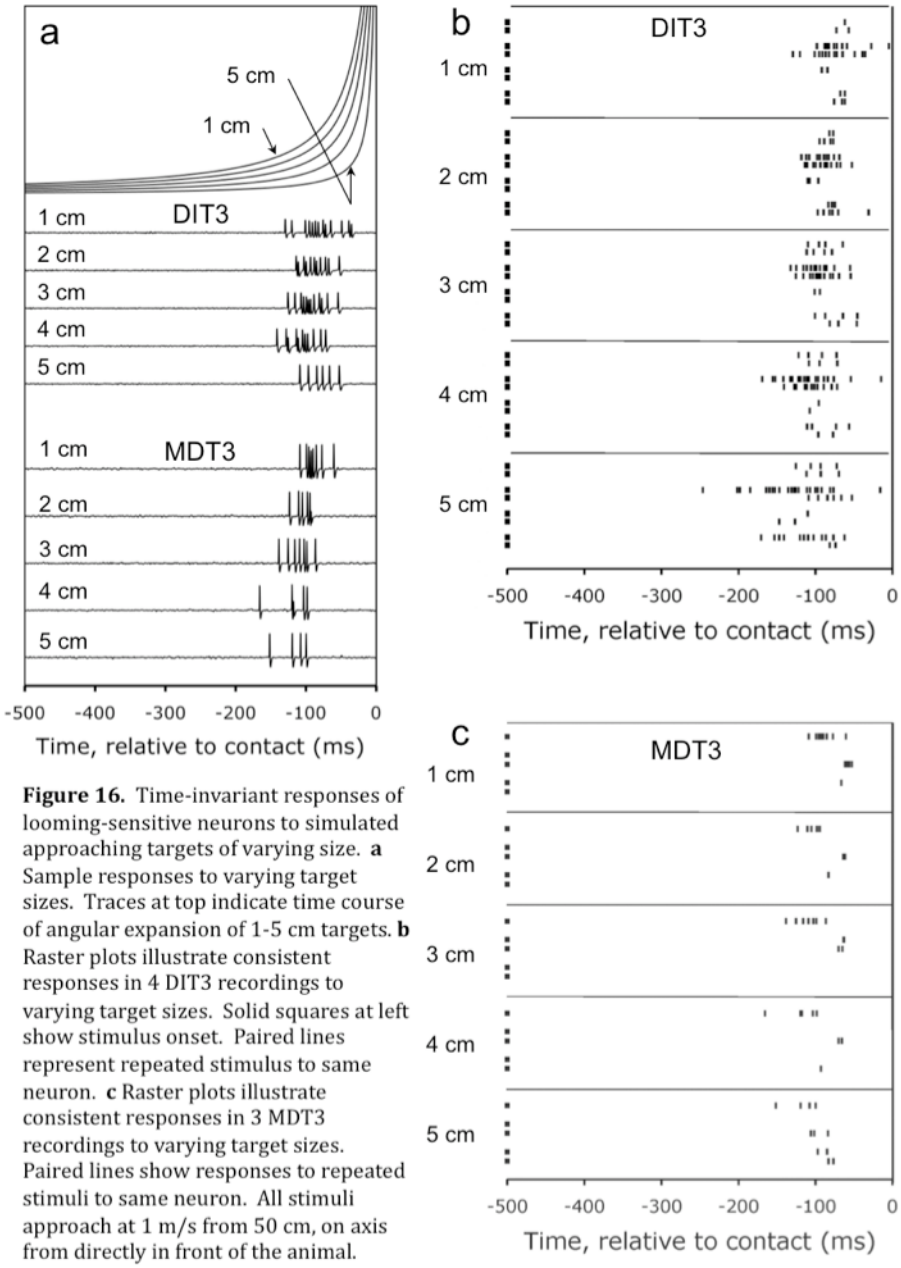

Figure 16. Time-invariant responses of looming-sensitive neurons to simulated approaching targets of varying size. **a** Sample responses to varying target sizes. Traces at top indicate time course of angular expansion of 1-5 cm targets. **b** Raster plots illustrate consistent responses in 4 DIT3 recordings to varying target sizes. Solid squares at left show stimulus onset. Paired lines represent repeated stimulus to same neuron. **c** Raster plots illustrate consistent responses in 3 MDT3 recordings to varying target sizes. Paired lines show responses to repeated stimuli to same neuron. All stimuli approach at 1 m/s from 50 cm, on axis from directly in front of the animal.

The timing of the looming-evoked burst was also relatively independent of the approach speed (Fig 17a). However there was a small tendency for both DIT3 and MDT3 to fire later with increasing speed (Fig 17). There was no consistent difference between the firing times of DIT3 (Fig 17b) and MDT3 (Fig 17c).

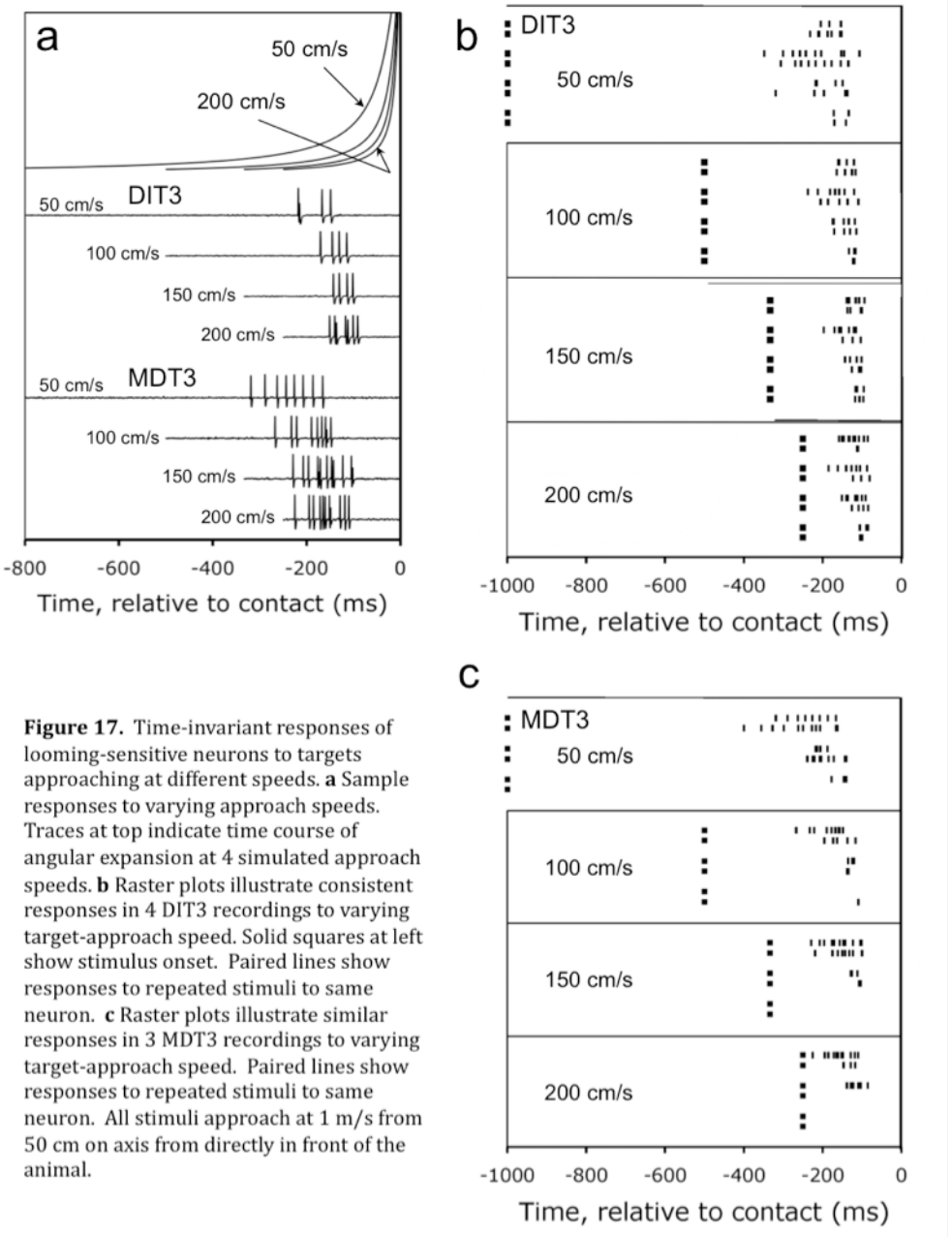

Figure 17. Time-invariant responses of looming-sensitive neurons to targets approaching at different speeds. **a** Sample responses to varying approach speeds. Traces at top indicate time course of angular expansion at 4 simulated approach speeds. **b** Raster plots illustrate consistent responses in 4 DIT3 recordings to varying target-approach speed. Solid squares at left show stimulus onset. Paired lines show responses to repeated stimuli to same neuron. **c** Raster plots illustrate similar responses in 3 MDT3 recordings to varying target-approach speed. Paired lines show responses to repeated stimuli to same neuron. All stimuli approach at 1 m/s from 50 cm on axis from directly in front of the animal.

For each neuron penetrated we obtained a receptive field profile by moving a 4° circular target along 7 parallel lines (spaced 10° apart) across the entire screen, in each of 4 directions (up, left, down, and right, in that order), a total of 28 stimulus presentations. The same series was then repeated with a 16° circular target. Unlike the other identified target-selective descending neurons (TSDNs), which are distinctly direction-selective, DIT3 and MDT3 showed responses to

targets moving in opposite directions, especially to both up and down movements (Figs. 18a and 19a). The receptive-field profiles shown in Figs. 18 and 19 were obtained with the 4° target, but the profiles obtained with the 16° target were very similar.

Both DIT3 and MDT3 responded vigorously to targets that deviated slightly from a collision course. We studied the dependence on the angle of object approach using a 1 cm diameter black circular target that began at a distance of 20 cm and moved at a speed of 40 cm/s along paths that deviated from a collision course by either 1° or 2°. DIT3 responded to deviations in all directions with a greater number of spikes to the 2° miss than to the 1° miss and a slight preference for targets missing to the left and below Fig(18c). MDT3 showed a strong directional preference for approaching objects whose trajectory deviated below or to the left (Fig 19c). For MDT3, it was typical to see very few or no spikes at all in response to 1° or 2° deviations toward the side contralateral to the recording electrode, even though a 1° deviation produces a path that differs from a direct hit only by 0.35 cm (i.e., the 1-cm target would still strike the head), and a 2° deviation misses by only 0.7cm (i.e., the target would miss by 2 mm).

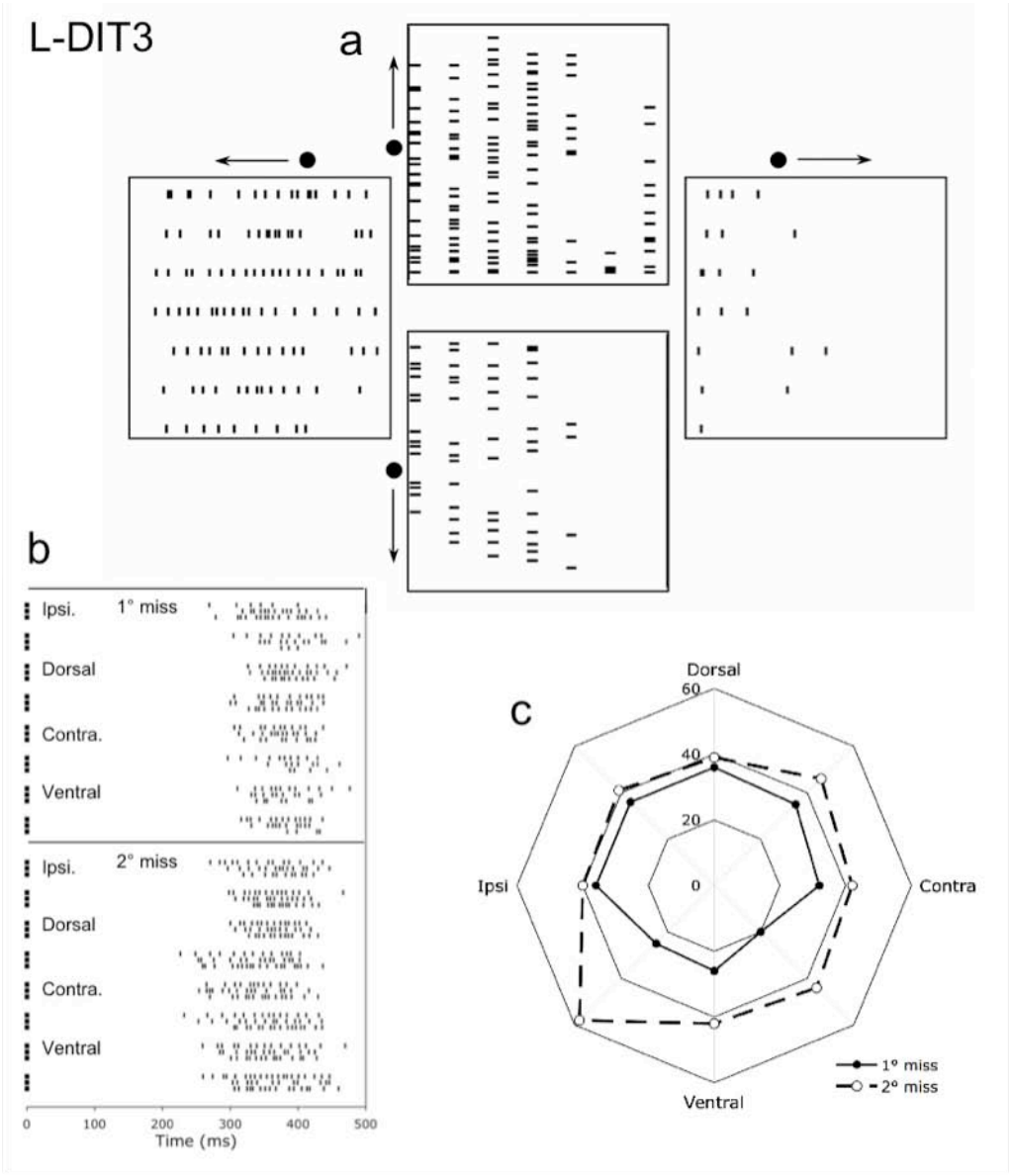

Figure 18. Spatial properties of looming-sensitive neuron, L-DIT3, in a Libellulid dragonfly **a** Receptive field plot. Line segments indicate spike locations as a 4° dark circular target was swept up, left, down, and right across the bright background display. **b** Raster plots show L-DIT3 responses to target deviating 1° (top) and 2° (bottom) from directly head on. Note greater responses and shorter spike latencies to 2° miss. Visual stimulus was 1 cm black disk expanding to simulate approach from 20 cm at 40 cm/s. **c** Polar plot of the total number of spikes over the 3 presentations for each miss-direction shown in **b**. Note somewhat greater response of L-DIT3 to a 2° miss to the lower left.

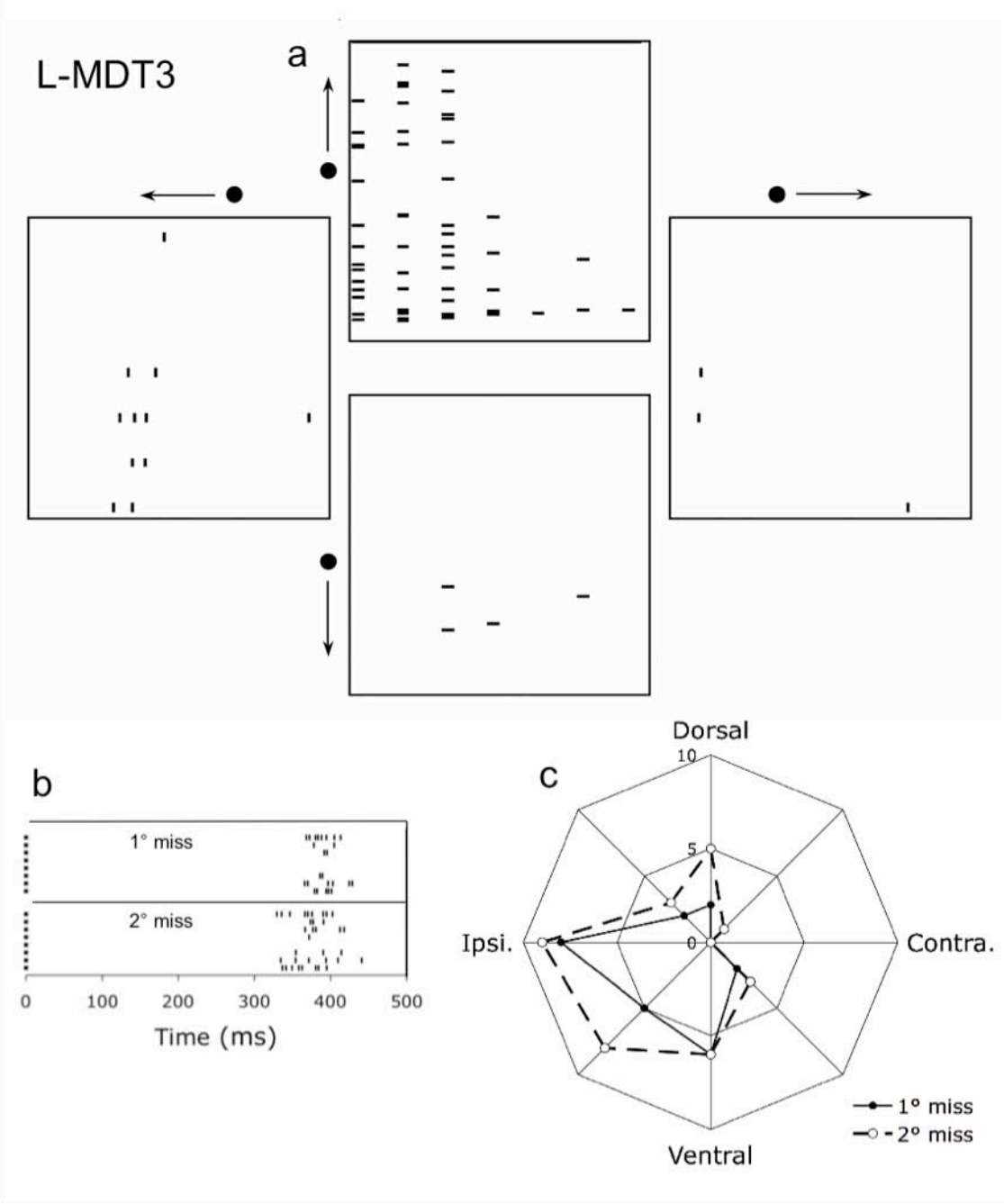

Figure 19. Spatial properties of looming-sensitive neuron, L-MDT3 in a Libellulid dragonfly. **a** Receptive field plot. Line segments indicate spike locations as a 4° dark circular target was swept up, left, down, and right across the bright background display. **b** Raster plots show L-DIT3 responses to target deviating from head-on by 1° (top) and 2° (bottom). Visual stimulus was 1 cm black disk expanding to simulate approach from 20 cm at 40 cm/s. Order of directions as in **Fig 5b** (i.e., first line is response to a miss to the left – ipsilateral- continuing clockwise around the circle). Note greater responses and shorter spike latencies to 2° miss. **c** Polar plot of the spike traces shown in b, showing strong preference of L-MDT3 to a misses downward and to the left.

Because calculation of time-to-contact requires information about the speed of an approaching object's expanding edges, we tested the ability of DIT3 and MDT3 to code target speed. Because of its larger receptive field and typically higher spike rate, DIT3 provided the better example of speed coding, i.e. higher spike rates and lower first-spike latencies with increasing speed (Fig. 20a). The tendency of this cell to habituate can be seen in the raster plot (Fig. 20b). Even with a 2-minute wait between the top half and the bottom half of the raster plot, the second series of stimuli elicited many fewer spikes and longer latencies. For this reason we separated the data from the two stimulus series in the plot of spike frequency as a function of target speed (Fig. 20c).

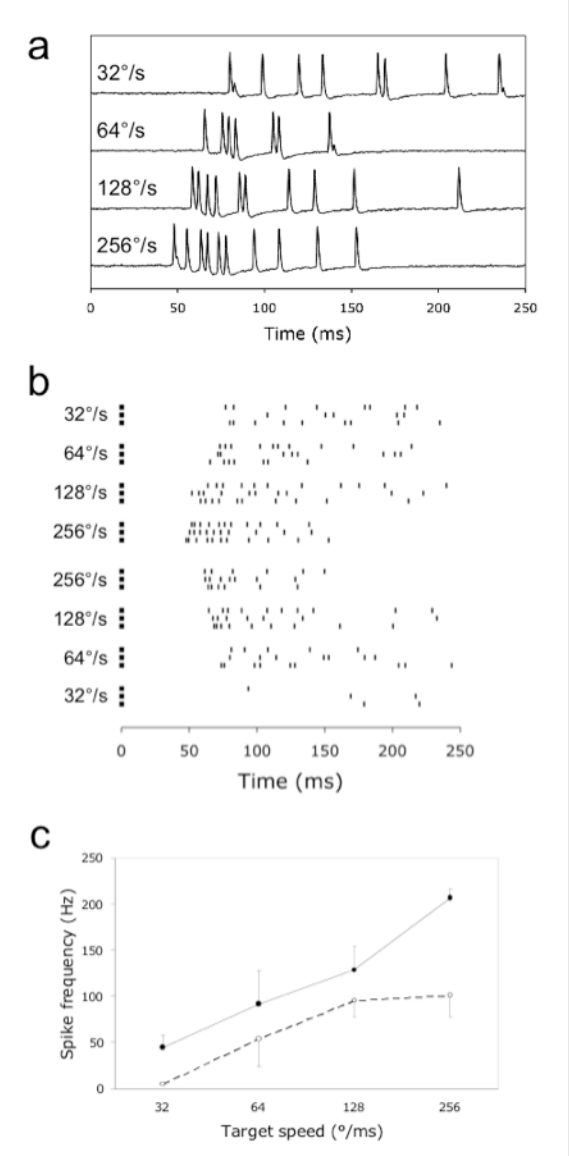

Figure 20. Responses of DIT3in a Libellulid dragonfly to speed of translating target. **a** Sample traces show increased spiking responses and shorter response latencies with increasing target speed. Traces are shown in order of presentation. **b** Raster plot shows responses in a single DIT3 recording to target moving at various speeds. For clarity the responses to the same speed have been grouped. A two-minute rest period separated the top and bottom series, but habituation was still readily apparent. **c** Average burst frequency as a function of target speed. Data from the raster plot (**b**), with the 2 stimulus series plotted separately. Error bars indicate one standard deviation from the mean.

Because MDT3 and DIT3 are already known to produce wing movements it was appropriate to consider their activity in the context of behavior (Olberg 1983). These looming sensitive neurons could serve an essential function in the

final stages of prey capture. High-speed video recordings of dragonfly prey-capture flights showed that about 20 ms before the foraging dragonfly makes contact with its prey, it began to extend its legs forward and upward to ensnare the prey (Olberg et al. 2007). This final ballistic behavior was much more tightly correlated with time-to-contact than with other variables such as the prey's distance or its size on the retina (Worthington and Olberg in prep). If DIT3 and MDT3 are involved in triggering this final segment of the prey-capture sequence, their activity might be expected to trigger movements of the legs as well as the wings. The heightened response to objects slightly off-axis could be responsible for correcting the dragonfly's final trajectory for successful capture. It is not yet known whether the legs can be thrust to the sides to compensate for an imperfect approach, but if so, the increased activity in response to objects missing on the preferred side could also play a role in this action. Determining the behavioral consequence of activity in these two looming sensitive neurons, DIT3 and MDT3, is the essential future direction in our investigation.

Prediction in the dragonfly visual system

The time-to-contact information contained in the spike traces from the looming sensitive TSDNs reflects one form of prediction in the signals descending from the dragonfly brain. Another form of prediction is shown by the TSDN spiking signals. In an information-theory analysis of TSDN responses, Adelman et al. (2003) showed that spikes of 2 TSDNs carry more information about future target location than about current on past position. The results of the outdoor receptive-field study confirmed this result and identified the two location-predicting TSDNs as DIT1 and MDT4. Figure 21 shows an example of this prediction in MDT4 (right panel), in contrast to MDT1 (left panel), whose spike trace does not predict location.

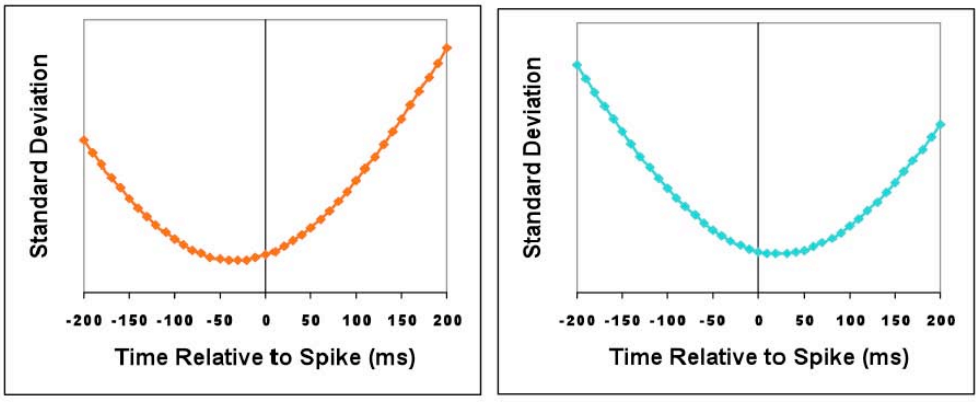

Figure 21. Receptive field size at various times relative to spikes for a non-predictive neuron (MDT1 – left panel) and a predictive neuron (MDT4 – right panel), both in the same Aeshnid dragonfly. Notice that the tightest receptive field for MDT4 (right) occurs 20 ms *after* the spike. This implies that the MDT4 spikes contain more information about the future position of the bead than about the present or past position. For MDT1 (left) the tightest receptive field is 30 ms after the spike, implying that spikes contain the most information about the recent position of the bead.

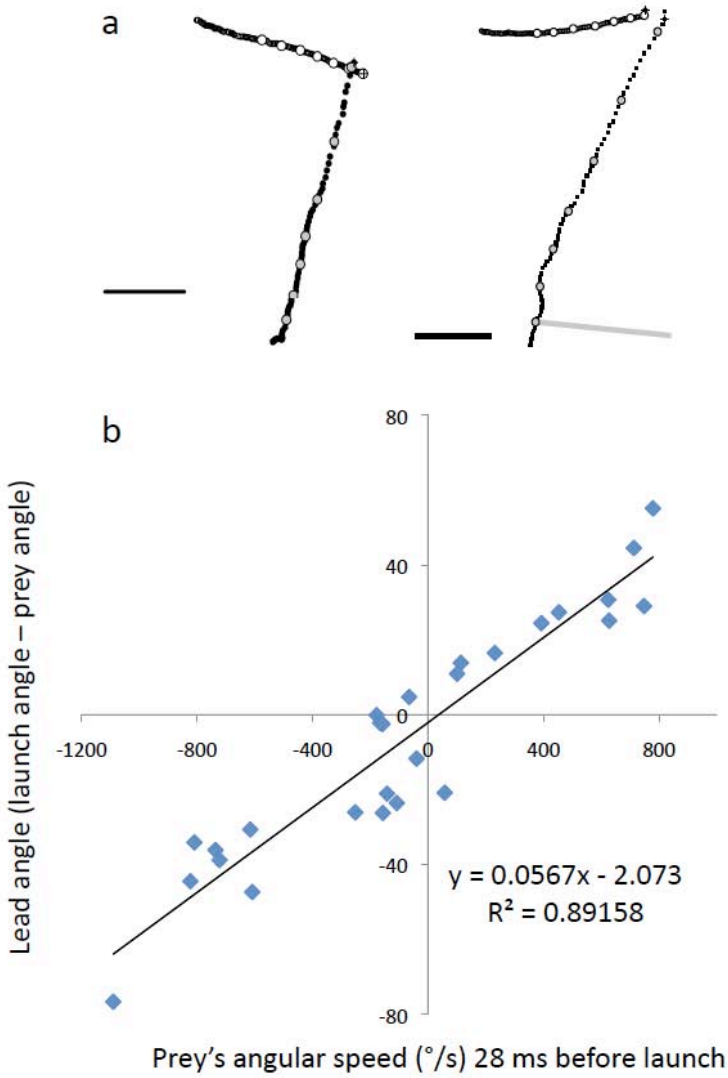

Figure 22. Calculation of interception angle by perched dragonflies. a. Example interception flight tracks (500 frames/s). Large filled circles mark head positions at 20 ms intervals. Left, dragonfly facing camera. Right, side view with gray bar indicating body orientation. Calibration bars, 2 cm. b. Lead angle (calculated as launch direction minus the direction to the prey 28 ms before takeoff) is a nearly linear function of angular speed 28 ms before takeoff.

Prey capture flight trajectories reflected the ability of the visual system to predict future prey location. Earlier work (Olberg et al. 2000) showed that dragonflies do not fly directly toward their prey, but rather aim at point in front of the prey, so that they intercept the prey with a relatively straight flight trajectory (Fig 22a). Prey capture flights are usually quite short, typically requiring only about 200 ms from takeoff to contact with the prey item. Perhaps because of this, evasive maneuvers by the prey insect have not been observed. Dragonflies are quite successful at capturing flying insects; Baird and May (1997) reported a capture rate of 76% in their study of foraging females (*Pachydiplax longipennis*), and a video study of males of various Libellullid

species foraging from pond's edge revealed only a single miss in 38 flights, a success rate of 97% (Olberg et al. 2000).

A key feature of the interception flight is takeoff toward the point of interception. Since takeoffs always lead the prey item (Fig 22b), the dragonfly must calculate takeoff direction using prior information about the angular velocity of the flying insect prey. To investigate this form of prediction, 28 takeoffs were selected in which the dragonfly's flight track was nearly linear after liftoff. The directions of these linear segments were plotted relative to the angular velocity of the prey at varying times before takeoff. The results of this analysis are shown in figure 22b, in which takeoff direction is plotted against angular velocity 28 ms prior to takeoff, the latency for which the r2 value of the relationship was the highest. These data suggest that (1) takeoff direction is a linear function the angular velocity of prey a short time before takeoff and (2) calculation of intended takeoff direction and transmission of a that information to the wings remarkably fast, requiring only about 28 ms.

Research at the JFRC

In June 2008, Olberg received a visiting scientist grant from the Janelia Farm Research Campus (JFRC) of the Howard Hughes Medical Institute (HHMI) to collaborate with Dr. Anthony Leonardo on visual motion analysis and flight control in dragonflies. The objective of this project is to record wirelessly from the TSDNs in free flight. A large fraction of Olberg's research time during the last two years has been invested in this project, which promises to elucidate, for the first time, the visual control of complex flight behavior in an insect (or any animal). Although the project was funded by HHMI, Olberg's grant from the AFOSR provided the teaching release that allowed him to spend extended periods of time at the JFRC in Ashburn, Virginia.

Dragonfly flight arena

The essential first step in this research effort was to develop an indoor flight arena in which dragonflies would perform natural behavior year round. Olberg and Leonardo designed a room (14 ft. X 18 ft., 15 ft ceiling) with a light system designed to mimic incident light from blue sky (Fig 23b). Ceramic metal halide lighting, augmented with UV, radiates upward into the room through UV transmitting acrylic windows surrounding the room just below the ceiling. The light is diffused and reflected by the white ceiling, resulting in light levels within the arena approximating daylight. One bank of lights is angled downward to mimic (somewhat) the point source of light provided by the sun. Temperature and humidity are controlled by systems designed to minimize air currents.

Since its opening in July 2008, the flight arena has gone through several iterations (Fig 23), each leading to more natural behavior and longer longevity for the dragonflies living in the arena. The present configuration has an artificial

turf floor, adjustable screens on the walls (allowing control of the visual horizon), large mesh clear screening about 10 ft above the floor, a small pond dropped down from a raised floor, permanent feeding stations where drosophila (fruit flies) are kept in

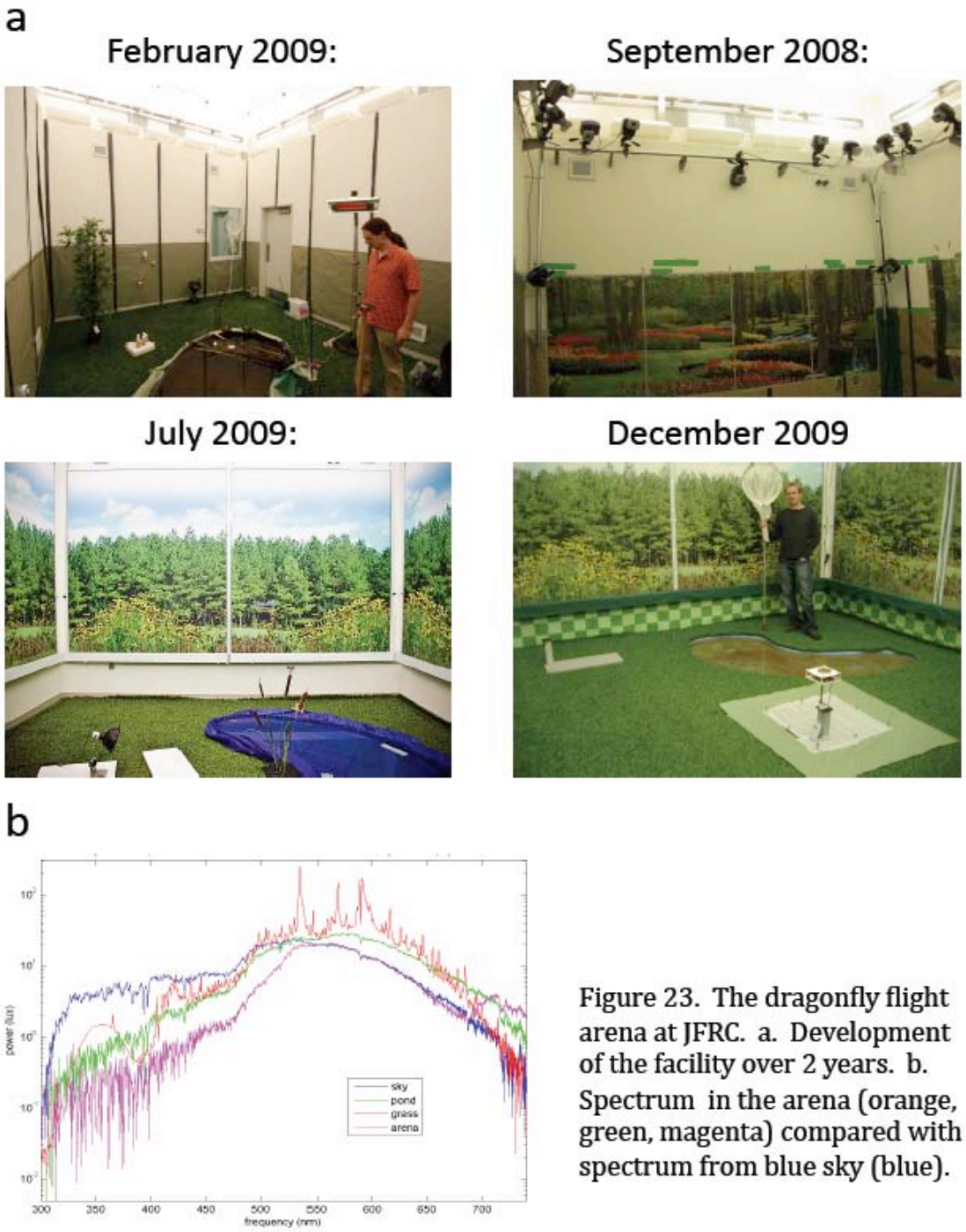

Figure 23. The dragonfly flight arena at JFRC. a. Development of the facility over 2 years. b. Spectrum in the arena (orange, green, magenta) compared with spectrum from blue sky (blue).

constant supply. A flat perch near the feeding station focuses most foraging flights on a volume of space viewed by 2 high-speed video cameras (Photron FastCam), mounted at right angles high on adjacent walls. Eighteen additional

high-speed cameras are mounted high on walls just below the light windows, each with an infrared light ring light surrounding the lens. These cameras sense reflective 1 mm beads mounted on the wings and head of the dragonfly, yielding 200 Hz motion analysis of flight dynamics in real time.

Lab-reared dragonflies survive in this environment for about 2 weeks. During this time their body mass doubles with the development of mature flight muscle. After about 2 weeks, as the dragonflies reach sexual maturity, a dispersing tendency results in the animals expending their energy reserves crashing into the walls and ceiling, ending their lives. However, for most of the time in the arena the dragonflies exhibit natural behavior, foraging successfully on the wing, consuming large numbers of drosophila. In short, the development of the flight arena has transformed the dragonfly into a tractable subject for laboratory experiments in behavior as well as electrophysiology.

Electrophysiology at JFRC

The amplifier/transmitter telemetry chip for the dragonfly project has been developed by Dr. Reid Harrison at the Univ. of Utah. The first versions were too heavy to be carried easily by the Libellulid dragonflies that behave well in the flight arena, but allowed checking of the technology (Fig 24). Recordings from

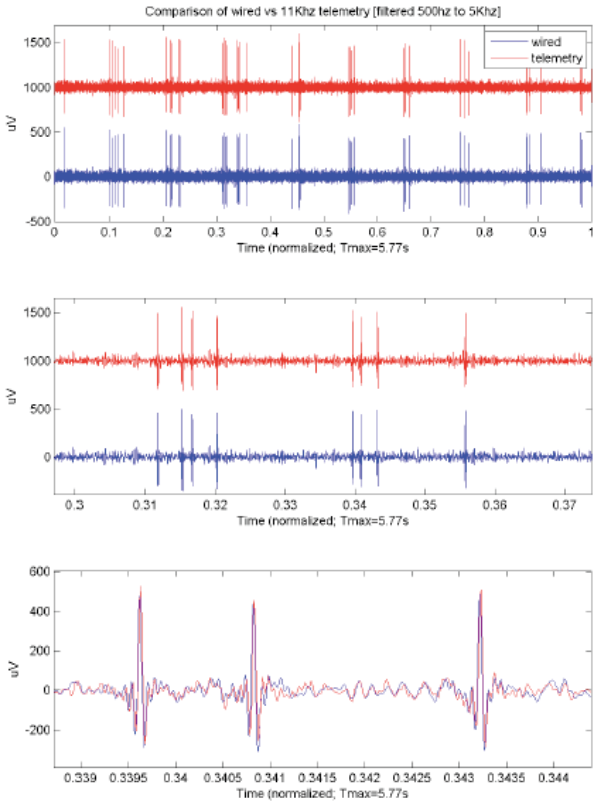

Figure 24. Test of the telemetry system. VNC signals recorded by electrode implanted in the mesothoracic ganglion of a Libellulid dragonfly showing easily sortable TSDN spikes. Red traces are signals amplified, transmitted and received by the telemetry system. Blue traces are recorded simultaneous with tether wires conducting the signal to a standard electrophysiology rig.

an earlier version of the chip is shown in Figure 24. A new, single battery 1.5 V chip is under development. This chip will weigh less than 200 mg; in pilot tests *Libellula lydia* foraged successfully in the arena carrying this mass. To reduce weight further, other methods of powering the chip are also under consideration.

TSDN signals have been successfully and reliably recorded using a multicontact silicone probe inserted into the mesothoracic ganglion (Fig 24). The probe is cemented to the sternal plate just anterior to the mesothoracic legs and fine wires lead from the probe to chip mounted to the ventral thorax behind the legs. This recording geometry yields high quality, sortable, multi-unit recordings of TSDN activity (Fig 24). A dragonfly with an implanted silicone probe exhibited normal flight in the arena. A follow-up experiment showed similar signal quality from the implanted electrode before and after flight.

A second approach to understanding the functioning of the TSDNs in dragonfly foraging behavior is to study the effect on the behavior of eliminating TSDNs individually or in groups. This will be accomplished by microelectrode injection of the fluorescent dye Lucifer Yellow into axons in the nerve cord of a minimally dissected animal. Dye injection is monitored with an epifluorescence stereo microscope mounted in the recording rig. The dragonfly is then moved to a 2-photon fluorescence microscope in which the injected axon is laser-ablated. After recovery from this operation the animal will be released in the flight arena for analysis of any defects in its flight behavior, especially in its visual prey-tracking ability.

The above electrophysiological approaches all require that the dragonfly be restrained, operated on, and subsequently released without harming its flight ability. To do this an immobilization unit (the "tomb") has been designed and built (Fig. 25). The milled aluminum "tomb" adjustably encloses the abdomen, thorax and outstretched wings without damaging them. It is mounted on a temperature-controlled plate so that the dragonfly's body temperature can be quickly varied. The dragonfly can be immobilized with cold for electrode placement and warmed to body temperatures of 30° or higher, as appropriate for visual receptive field studies. Dragonflies have shown apparently normal behavior after minimal surgery and recording in the tomb.

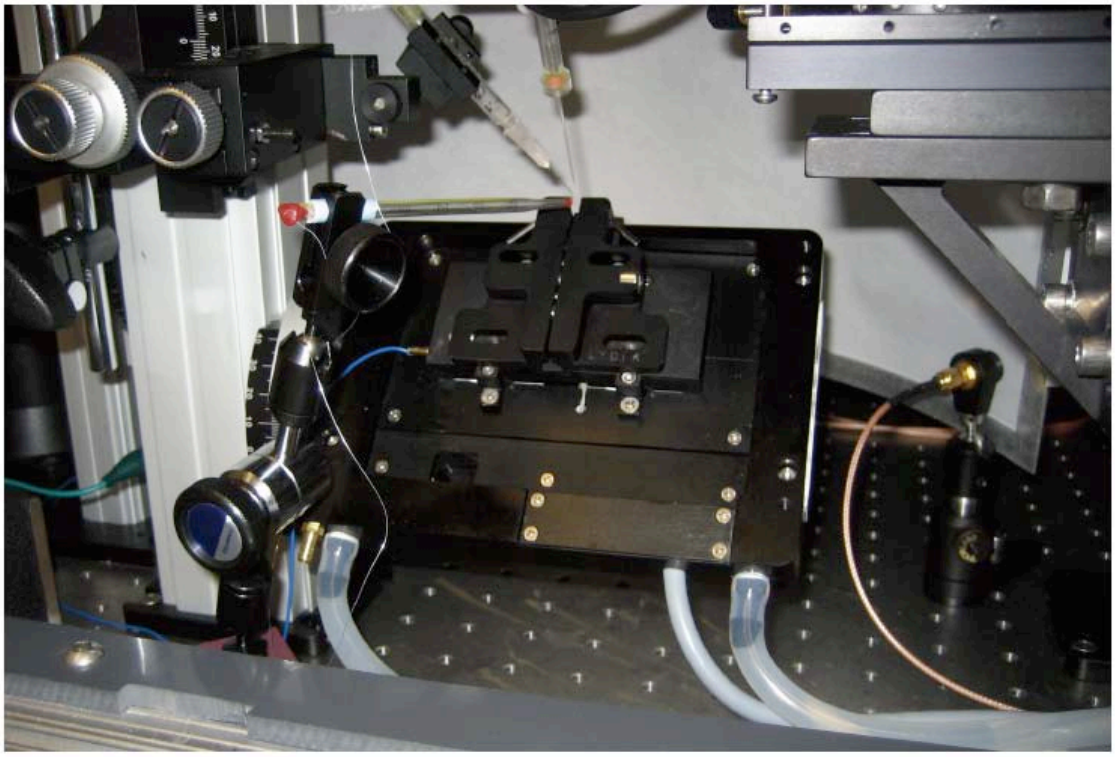

Figure 25. "The tomb," a temperature controlled dragonfly restraint apparatus for electrode placement and receptive field studies, developed in collaboration with Dr. Leonardo at the JFRC. Animals can be immobilized for hours in the apparatus without deleterious effects on flight behavior after release.

In summary, from Dr. Olberg's collaborative research efforts with Dr. Leonardo at the JFRC, all the technology has been developed for successful recording of the target selective neurons during free foraging flight. Dragonflies are showing natural foraging behavior in the JFRC flight arena. The dragonflies fly normally with the implanted silicone probe. The silicon probe reliably picks up TSDN spiking signals. The telemetry chip and receiver yield high quality electrophysiological records. They are able to forage successfully carrying the telemetry "bellypack". Wireless recordings of TSDN activity during foraging flight will commence in early summer 2010.

References

Adelman, TL, Bialek, W and Olberg, RM (2003) The information content of receptive fields. (Neuron 40:823-833)

Baird JM, May ML (1997) Foraging behavior of *Pachydiplax longipennis* (Odonata: Libellulidae). J Insect Behavior 10: 655-678

Frye MA, Olberg RM (1995) Visual receptive field properties of feature detecting neurons in the dragonfly. J Comp Physiol A 177: 569-576

Olberg RM, Worthington AH, Venator KR (2000) Prey pursuit and interception in dragonflies. J Comp Physiol A 186:155-162
Olberg RM (1983) Identified interneurons steer flight in the dragonfly. Soc Neurosci Abstr 9: 326
Olberg RM (1986) Identified target-selective visual interneurons descending from the dragonfly brain. J Comp Physiol A 159:827-840
Olberg RM, Seaman RC, Coats MI, Henry AF (2007) Eye movements and target fixation during dragonfly prey-interception flights. J Comp Physiol A 193:685–693
Worthington A, Olberg R (2009) Looming-sensitive neurons in the dragonfly predict time to contact with prey. Abst. 6th International Congress of Odonatology.